END

FILMED

3-84

DTIC

MICROCOPY RESOLUTION TEST CHART

Canadä

AD A137690

IMPLEMENTATION OF NISITANI'S BODY FORCE METHOD FOR THE SOLUTION OF NOTCH PROBLEMS
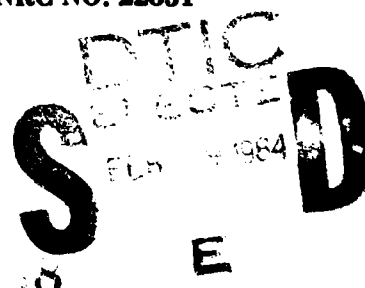
by

W. E. Fraga, R. L. Hewitt

National Aeronautical Establishment

National Research
Council Canada
Conseil national
de recherches Canada

NATIONAL AERONAUTICAL ESTABLISHMENT

SCIENTIFIC AND TECHNICAL PUBLICATIONS

AERONAUTICAL REPORTS:

Aeronautical Reports (LR): Scientific and technical information pertaining to aeronautics considered important, complete, and a lasting contribution to existing knowledge.

Mechanical Engineering Reports (MS): Scientific and technical information pertaining to investigations outside aeronautics considered important, complete, and a lasting contribution to existing knowledge.

AERONAUTICAL NOTES (AN): Information less broad in scope but nevertheless of importance as a contribution to existing knowledge.

LABORATORY TECHNICAL REPORTS (LTR): Information receiving limited distribution because of preliminary data, security classification, proprietary, or other reasons.

Details on the availability of these publications may be obtained from:

Publications Section,
National Research Council Canada,
National Aeronautical Establishment,
Bldg. M-16, Room 204,
Montreal Road,
Ottawa, Ontario
K1A 0R6

ÉTABLISSEMENT AÉRONAUTIQUE NATIONAL

PUBLICATIONS SCIENTIFIQUES ET TECHNIQUES

RAPPORTS D'AÉRONAUTIQUE

Rapports d'aéronautique (LR): Informations scientifiques et techniques touchant l'aéronautique jugées importantes, complètes et durables en termes de contribution aux connaissances actuelles.

Rapports de génie mécanique (MS). Informations scientifiques et techniques sur la recherche externe à l'aéronautique jugées importantes, complètes et durables en termes de contribution aux connaissances actuelles.

CAHIERS D'AÉRONAUTIQUE (AN): Informations de moindre portée mais importantes en termes d'accroissement des connaissances.

RAPPORTS TECHNIQUES DE LABORATOIRE (LTR): Informations peu disséminées pour des raisons d'usage secret, de droit de propriété ou autres ou parce qu'elles constituent des données préliminaires.

Les publications ci-dessus peuvent être obtenues à l'adresse suivante:

Section des publications
Conseil national de recherches Canada
Établissement aéronautique national
Im. M-16, pièce 204
Chemin de Montréal
Ottawa (Ontario)
K1A 0R6

IMPLEMENTATION OF NISITANI'S BODY FORCE METHOD FOR THE SOLUTION OF NOTCH PROBLEMS

APPLICATION DE LA MÉTHODE DES FORCES DE NISITANI POUR RÉSOUDRE DES PROBLÈMES D'ENTAILLES ET DE FISSURES

by/par

W.E. Fraga*, R.L. Hewitt

National Aeronautical Establishment

* Department of Mathematics, University of Alberta

W. Wallace, Head/Chef
Structures and Materials Laboratory/
Laboratoire des structures et matériaux

G.M. Lindberg
Director/Directeur

SUMMARY

An outline of Nisitani's body force method is presented and details of the numerical implementation provided. Full details are provided for the solution of several problems including single cracks or single elliptical notches in semi-infinite plates as well as the problem of an embedded crack near a semi-elliptical notch in a semi-infinite plate.

RÉSUMÉ

Une description de la méthode des forces de Nisitani avec des exemples numériques est présentée dans cette note. Les exemples de résolution de problèmes sont très détaillés et comprennent notamment des problèmes de fissures uniques ou d'entailles elliptiques uniques dans des plaques semi-infinies ainsi que le problème d'une fissure située à proximité d'une entaille semi-elliptique dans une plaque semi-infinie.

(iii)

CONTENTS

CONTENTS (Cont'd)

TABLES

ILLUSTRATIONS

APPENDICES

IMPLEMENTATION OF NISITANI'S BODY FORCE METHOD

FOR THE SOLUTION OF NOTCH PROBLEMS

1.0 INTRODUCTION

Efficient use of fracture mechanics methods for damage tolerance assessments depends upon knowledge of the stress intensity factor for the flaw considered. While these are available for some simple crack geometries, it is often necessary either to resort to some approximation or employ a complex finite element program to obtain the information. Alternatively, a boundary integral approach may be used which may in some cases be more efficient.

One such approach is the body force method proposed by Nisitani[1]. This is a relatively straightforward technique in principle which makes use of the stress field derived from point forces acting in an infinite plate or body. Boundary conditions are satisfied by applying body forces (continuously embedded point forces) along the edges of notches or cracks (the density of these body forces being determined from the boundary conditions). The method is applicable to both two and three dimensional problems.

In attempting to use this method following the work of Nisitani, it was found that certain details of the technique were absent or available only in the Japanese literature, and it therefore seems appropriate that, having implemented the method at NRC, the details of the implementation be reported. Thus for the particular problems studied, all the relevant information from various papers of Nisitani have been brought together and all the details necessary for implementation are given in this report. An additional report[2] is available on request which contains listings of the computer programs developed with appropriate documentation.

2.0 PRINCIPLES OF BODY FORCE METHOD

In order to make this report more complete, a brief review of the principles of the body force method will be presented. The review follows that of Nisitani[1] but various points which were found difficult to follow have been amplified while others which were considered to be unnecessary for a general understanding of the method have been omitted.

2.1 Tension of Infinite Plate with an Elliptic Hole

Consider the problem of an elliptical hole in an infinite plate as shown in Figure 1. If a stress, σ_x^∞, is applied at infinity, the x and y components of the displacement, u and v, at an arbitrary point (ξ, η) on the edge of the hole are independent of the Poisson's ratio, ν, and are given by[3]:

$$u = \frac{\sigma_x^\infty}{E} (1 + 2b/a) \, \xi \tag{1a}$$

and

$$v = -\frac{\sigma_x^\infty}{E} \eta \tag{1b}$$

where E is the Young's modulus and b and a are the semi-major and semi-minor widths respectively of the ellipse.

Now consider an elliptical plate of the same size and shape as the hole. For the displacements on the edge of this plate to be the same as for the edge of the hole, the strain components at an arbitrary point on the plate must be

$$\epsilon_x = \frac{\partial u}{\partial \xi} = \frac{\sigma_x^\infty}{E} (1 + 2b/a) \tag{2a}$$

$$\epsilon_y = \frac{\partial v}{\partial \eta} = -\frac{\sigma_x^\infty}{E} \tag{2b}$$

and
$$\gamma_{xy} = 0 \tag{2c}$$

where ϵ and γ are the normal and shear strains respectively. From Hooke's law, the normal and shear stress, σ and τ, corresponding to these strains are

$$\sigma_x = \frac{E}{1 - \nu^2} (\epsilon_x + \nu \epsilon_y) = \frac{\sigma_x^\infty}{1 - \nu^2} (1 + 2b/a - \nu) \tag{3a}$$

$$\sigma_y = \frac{E}{1 - \nu^2} (\epsilon_y + \nu \epsilon_x) = \frac{-\sigma_x^\infty}{1 - \nu^2} (1 - \nu (1 + 2b/a)) \tag{3b}$$

$$\tau_{xy} = G\gamma_{xy} = 0 \tag{3c}$$

The elliptical plate having these surface stresses can be inserted exactly into the infinite plate with the elliptical hole subjected to a stress σ_x^∞, producing an infinite plate with no hole. Therefore the problem of an infinite plate with a hole is equivalent to the problem of an infinite plate with no hole, but having the stresses given by Equations (3) applied along the imaginary boundary of the ellipse as shown in Figure 2. These stresses are obtained from a series of continuously embedded point forces along the boundary.

The densities, ρ_x and ρ_y, of these body forces in the x and y directions can be obtained from Equations (3) as

$$\rho_x = \frac{\sigma_x^\infty}{1 - \nu^2} (1 + 2b/a - \nu) \tag{4a}$$

and
$$\rho_y = \frac{-\sigma_x^\infty}{1 - \nu^2} (1 - \nu (1 + 2b/a)) \tag{4b}$$

where 'unit length' is measured in y direction for ρ_x and in x direction for ρ_y.

Since ν does not affect the end results according to Nisitani[1], it may be set to zero and the body forces written

$$\rho_x = \sigma_x^\infty (1 + 2b/a) \tag{5a}$$

and

$$\rho_y = -\sigma_x^\infty \tag{5b}$$

Thus for an elliptical hole in an infinite plate the densities of body force are constant along the boundary of the hole. In general, however, they will not be constant and a numerical technique must be used to determine them.

2.2 Tension of Infinite Plate with a Crack

The case of an infinite plate with a crack under tension is shown in Figure 3. A crack can be considered as an extremely slender elliptical hole. As b/a tends to infinity, the hole becomes a crack and the points at which body forces are applied come closer to each other. Thus the fundamental stress field is obtained from a pair of point forces equal in magnitude and opposite in direction.

To find the stress at an arbitrary point (x, y) due to a pair of point forces separated by a distance δ from each other, consider Figure 4. The stress at (x,y) in the x direction due to the body forces X acting on the element $d\eta$ may be written

$$\sigma_x = X \sigma_x^X (\xi,\eta,x,y)\Big|_{X=1}$$

$$- X \sigma_x^X (\xi - \delta,\eta,x,y)\Big|_{X=1} \tag{6}$$

where σ_x^X is the stress in the x direction at (x,y) due to a unit body force in the x-direction at (ξ,η). This may be written

$$\sigma_x \simeq X \frac{\partial \sigma_x^X}{\partial \xi}\bigg|_{X=1} \cdot \delta$$

$$= \frac{\partial \sigma_x^X}{\partial \xi}\bigg|_{x} \quad (X\delta) \tag{7}$$

But the point force X can be written

$$X = \rho_x \, d\eta \tag{8}$$

and for the very slender ellipse (i.e. small ξ)

$$\delta = 2\xi \tag{9}$$

Therefore, substituting Equations (8) and (9) into (7)

$$\sigma_x = \left. \frac{\partial \sigma_x^X}{\partial \xi} \right|_{X=1} (\rho_x \, d\eta \, 2\xi)$$

or

$$d\sigma_x = \lim_{\xi \to 0} \left[(\rho_x d\eta) \left. \frac{\partial \sigma_x^X}{\partial \xi} \right|_{X=1} 2\xi \right]$$

$$= \left. \frac{\partial \sigma_x^X}{\partial \xi} \right|_{\substack{X=1 \\ \xi=0}} \rho_x \, 2\xi \left. \right|_{\xi \to 0} d\eta \tag{10}$$

But for an ellipse

$$\frac{\xi^2}{a^2} + \frac{\eta^2}{b^2} = 1$$

or

$$\xi = \frac{a}{b} \sqrt{b^2 - \eta^2} \tag{11}$$

and from Equation (5a)

$$\rho_x = \sigma_x^\infty (1 + 2b/a) \tag{5a}$$

Thus substituting Equations (5a) and (11) in (10)

$$d\sigma_x = \left. \frac{\partial \sigma_x^X}{\partial \xi} \right|_{\substack{X=1 \\ \xi=0}} \cdot 4\sigma_x^\infty \sqrt{b^2 - \eta^2} \, d\eta \tag{12}$$

From the fundamental stress field for a point force acting in an infinite plate (see Appendix 1)

$$\sigma_x^X = \frac{-(x-\xi)(3(x-\xi)^2 + (y-\eta)^2)}{4\pi((x-\xi)^2 + (y-\eta)^2)^2} X \tag{13}$$

therefore

$$\frac{\partial \sigma_x^X}{\partial \xi}\Bigg|_{\substack{X=1 \\ \xi=0}} = \frac{-3x^4 + 6x^2(y-\eta)^2 + (y-\eta)^4}{4\pi(x^2 + (y-\eta)^2)^3} \tag{14}$$

To determine the stress at an arbitrary point $(0,y)$ on the y axis (i.e. on the crack line) Equation (12) must be integrated and added to the uniform stress at infinity σ_x^∞, i.e.

$$\sigma_x(y) = \lim_{x \to 0}\left[\int_{-b}^{b} \frac{(-3x^4 + 6x^2(y-\eta)^2 + (y-\eta)^4)}{4\pi(x^2 + (y-\eta)^2)^3} \left(4\sigma_x^\infty \sqrt{b^2 - \eta^2}\right) d\eta \right] + \sigma_x^\infty \tag{15}$$

When $|y| > b$, i.e. beyond the crack, x may be set to zero directly and Equation (15) may be written

$$\sigma_x(y) = \frac{\sigma_x^\infty}{\pi} \int_{-b}^{b} \frac{\sqrt{b^2 - \eta^2}}{(y-\eta)^2} d\eta + \sigma_x^\infty$$

$$= \frac{\sigma_x^\infty}{\pi}\left[\frac{\sqrt{b^2 - \eta^2}}{y - \eta} - \sin^{-1}\frac{\eta}{b} + \frac{|y|}{\sqrt{y^2 - b^2}}\sin^{-1}\left[\frac{y\eta - b^2}{b(y-\eta)}\right]\right]_{-b}^{b} + \sigma_x^\infty$$

$$= \frac{|y|\,\sigma_x^\infty}{\sqrt{y^2 - b^2}}$$

$$\simeq \frac{\sigma_x^\infty \sqrt{\pi b}}{\sqrt{2\pi r}} \qquad \text{for } r = |y| - b \ll b \tag{16}$$

or

$$\sigma_x(y) = \frac{K_1}{\sqrt{2\pi r}} \tag{17}$$

where K_1 is the mode 1 stress intensity factor

For $|y| < b$ and $x = 0$, the integral contains a singularity at $y = \eta$, so principal values must be taken to evaluate it. Denoting the integrand as $f(\eta)$, Equation (15) may be written

$$\sigma_x(y) = \lim_{x \to 0} \int_{-b}^{b} f(\eta)\, d\eta + \sigma_x^\infty$$

$$= \lim_{x \to 0} \left[\int_{-b}^{y-\epsilon} f(\eta)\, d\eta + \int_{y+\epsilon}^{b} f(\eta)\, d\eta \right]$$

$$+ \lim_{x \to 0} \int_{-\epsilon}^{\epsilon} f(\eta)\, d\eta + \sigma_x^\infty \tag{18}$$

The first two integrals contain no singularities and may be integrated directly by setting $x = 0$. The result is[1] for $|\epsilon| \ll b$:

$$\lim_{x \to 0} \left[\int_{-b}^{y-\epsilon} f(\eta)\, d\eta + \int_{y+\epsilon}^{b} f(\eta)\, d\eta \right] = \Big[F(y-\epsilon) - F(-b) + F(b) - F(y+\epsilon) \Big]$$

$$\simeq \frac{\sigma_x^\infty}{\pi} \left[\frac{2\sqrt{b^2 - y^2}}{\epsilon} \right] - \sigma_x^\infty \tag{19}$$

in which

$$F(\eta) = \frac{\sigma_x^\infty}{\pi} \int \frac{\sqrt{b^2 - \eta^2}}{(y - \eta)^2}\, d\eta$$

$$= \frac{\sigma_x^\infty}{\pi} \left[\frac{\sqrt{b^2 - \eta^2}}{y - \eta} - \sin^{-1}\left(\frac{\eta}{b} \right) \right.$$

$$\left. + \frac{y}{\sqrt{b^2 - y^2}} \ln \left| \frac{(b^2 - y\eta) + \sqrt{(b^2 - y^2)(b^2 - \eta^2)}}{b(y - \eta)} \right| \right] \tag{20}$$

The third integral contains a singularity when $x = 0$, so it is not permissible to set $x = 0$ before performing the integration. The integration must be performed first before the limit is taken. For $\epsilon \ll b$, $\sqrt{b^2 - \eta^2}$ may be approximated by $\sqrt{b^2 - y^2}$ which may then be taken outside the integral. Then setting $t = y - \eta$

$$\lim_{x \to 0} \int_{y-\epsilon}^{y+\epsilon} f(\eta)\, d\eta \simeq \lim_{x \to 0} \left[\frac{\sigma_x^\infty}{\pi} \sqrt{b^2 - y^2} \int_{-\epsilon}^{\epsilon} \frac{-3x^4 + 6x^2 t^2 + t^4}{(x^2 + t^2)^3}\, dt \right]$$

$$= \lim_{x \to 0} \left[\frac{-2\sigma_x^\infty}{\pi} \sqrt{b^2 - y^2} \left\{ \frac{\epsilon}{x^2 + \epsilon^2} + \frac{2x^2 \epsilon}{(x^2 + \epsilon^2)^2} \right\} \right]$$

$$= - \frac{2\sigma_x^\infty}{\pi \epsilon} \sqrt{b^2 - y^2} \tag{21}$$

Substituting Equations (19) and (21) into (18) yields the result

$$\sigma_x(y) = 0 \qquad \text{for} \qquad |y| < b \tag{22}$$

Equations (22) and (17) show that the problem of an infinite plate with a crack can be reduced to that of an infinite plate without a crack but subjected to body forces along the imaginary crack line. The stresses at an arbitrary point are obtained by integrating the stress field for a pair of point forces.

It is also clear from examination of Equation (20) that the same result would be obtained by ignoring the singularity, and in fact no special consideration is necessary when integrating these expressions analytically.

The strength, dR, of a pair of point forces has been expressed as the product of the magnitude of the forces, X, and the distance between them, δ,

i.e. $$dR = X\delta$$

or, from Equations (8) and (9)

$$dR = \rho_x\, d\eta\, 2\xi \Big|_{\xi \to 0}$$

Then the density of a pair of point forces, $dR/d\eta$, is obtained as

$$\frac{dR}{d\eta} = (\rho_x 2\xi) \Big|_{\xi \to 0} \tag{22}$$

which for a crack in an infinite plate may be written using Equations (5a) and (11) as

$$\frac{dR}{d\eta} = 4\sigma_x^\infty \sqrt{b^2 - \eta^2} \tag{23}$$

However, for convenience, Nisitani[1], has defined a quantity, γ, which for the crack in the infinite plate is given by

$$\gamma = \frac{1}{4\sqrt{b^2 - \eta^2}} \cdot \frac{dR}{d\eta} \qquad (24)$$

and which he calls the density of a pair of body forces.

(The reason for using this quantity, rather than $dR/d\eta$ directly, is that the variation in γ along the crack line for general problems will then be small, and so setting $\gamma = $ constant within an interval will result in an accurate solution).

Comparing Equations (23) and (24), for the crack in an infinite plate, γ is constant and equal to σ_x^∞. Thus from Equation (17)

$$K_1 = \gamma\sqrt{\pi b} \qquad (25)$$

For other crack problems, the densities of pairs of body forces γ will not be constant, but will vary along the crack. For these problems a numerical method must be used to determine the densities of body forces at the tips of the cracks γ_A and γ_B. From these the stress intensity factors K_{1A} and K_{1B} at each tip can be calculated according to Nisitani[1] as

$$K_{1A} = \gamma_A \sqrt{\pi b}$$

$$(26)$$

$$K_{1B} = \gamma_B \sqrt{\pi b}$$

3.0 NUMERICAL TECHNIQUE

3.1 Crack in a Semi-infinite Plate

3.1.1 Formulation

Consider the case of a crack in a semi-infinite plate under tension as shown in Figure 5. Whereas in an infinite plate the densities of pairs of body forces, γ, were constant along the crack, here the densities vary continuously.

If the crack is divided into MM equal intervals and γ is set constant within each interval, a stepped distribution will result which will be accurate for large values of MM. The derivative of the stress field due to a point force in a semi-infinite plate is used to determine the stresses at the mid-point of each interval due to the body forces and the boundary conditions that the mid-point of each interval be free of stress are applied. The densities of the pair of body forces in each interval can then be determined.

The stress intensity factors at both tips of the crack can be calculated using only the densities γ_1 and γ_{MM} at the ends of the crack. The stresses at an arbitrary point on the plate can be found by taking a linear combination of the body force densities.

3.1.2 Solution Sequence

(1) The crack AB is divided into MM intervals, with the end points of the N-th intervals having values of η of

$$\eta_{N-1} = e - b + 2(N-1)b/MM$$

$$\eta_N = e - b + 2Nb/MM$$

where b is the half length of the crack and e the distance from the centre of the crack to the edge of the plate as shown in Figure 5. The mid-point of the M-th interval has a co-ordinate, y of

$$y_M = e - b + (2M - 1)b/MM$$

(2) The influence coefficient $\sigma_{xM}^{\gamma N}$, which is the stress at the mid-point of the M-th interval due to a pair of body forces on the N-th interval having a density $\gamma_N = 1$, is given by

$$\sigma_{xM}^{\gamma N} = \int\limits_{\substack{N\text{-th} \\ \text{interval}}} \left.\frac{\partial \sigma_x^X}{\partial \xi}\right|_{\substack{X=1 \\ x=\xi=0}} \cdot 4\sqrt{b^2 - (\eta - e)^2}\ d\eta$$

Using the fundamental stress field for a point force acting in a semi-infinite plate [Appendix 1] this may be written

$$\sigma_{xM}^{\gamma N} = \int\limits_{\eta_{N-1}}^{\eta_N} \left[\frac{1}{(y-\eta)^2} - \frac{1}{(y+\eta)^2} + \frac{12y}{(y+\eta)^3} - \frac{12y^2}{(y+\eta)^4} \right] \cdot \frac{1}{\pi} \cdot \sqrt{b^2 - (\eta - e)^2}\ d\eta$$

This integral can be solved either analytically (see 3.1.3 and 3.1.5) or numerically, with the singularity treated in the same manner as for the infinite plate.

(3) The boundary conditions are applied to make the mid-point of each interval free of stress, i.e.

$$\sum_{N=1}^{MM} \gamma_N \sigma_{xM}^{\gamma N} + \sigma_x^\infty = 0 \qquad \text{for } M = 1, 2 \ldots MM$$

This results in a system of MM linear equations in MM unknowns, γ_N, which can be solved using a matrix inversion routine.

(4) The stress intensity factors K_{1A} and K_{1B} are then calculated from γ_1 and γ_{MM} as

$$K_{1A} = \gamma_1 \sqrt{\pi b} \qquad \text{and} \qquad K_{1B} = \gamma_{MM} \sqrt{\pi b}$$

(5) The stress at an arbitrary point P on the plate can be calculated from the influence coefficients for that point and the body force densities, i.e.

$$\sigma_{xP} = \sum_{N=1}^{MM} \gamma_N \, \sigma_{xP}^{\gamma N} + \sigma_x^{\infty}$$

(6) For finite values of MM there will be errors in K_{1A} and K_{1B} because of the approximation of a stepped distribution. The true values of K_{1A} and K_{1B} correspond to MM = ∞. Since Nisitani has shown the error to be proportional to 1/MM these values can be obtained by extrapolation from two values of MM such as 12 and 24.

3.1.3 Analytic Integration

The integral in 3.1.2 in the calculation of $\sigma_{xM}^{\gamma N}$ was performed analytically. The result is shown in Appendix 2. Although the integral involves a singular term in the case where M = N, no special consideration is required as illustrated earlier.

3.1.4 Results (Analytic Integration)

Table I compares the correction factors, F_{1A}, obtained in the present investigation with those of Nisitani[1] for various values of the number of intervals MM, for a crack with a b/e ratio of 0.5.

TABLE I

CRACK IN SEMI-INFINITE PLATE

MM	F_{1A} (this work)	F_{1A} (Nisitani)
12	1.090367	1.09033
16	1.090622	1.09063
24	1.090919	1.09091
32	1.091024	1.09104
48	1.091243	1.09115

b/e = 0.5

$$F_{1A} = \frac{K_{1A}}{\sigma_x^{\infty} \sqrt{\pi b}}$$

The agreement is very good and the minor discrepancies can be attributed to computer differences.

The correction factor F_{1A} is plotted against 1/MM in Figure 6. The error in F_{1A} is almost linear with respect to 1/MM, with the value of F_{1A} tending to 1.09149 as MM tends to infinity. This compares with the value of 1.0914 obtained by Nisitani[1].

3.1.5 Numerical Integration

For most problems, the integral for the influence coefficients cannot be integrated analytically as in 3.1.3 and the integration must be performed numerically. To check on suitable parameters for these integrations, the integral of 3.1.2 used to evaluate $\sigma_{xM}^{\gamma N}$ was also solved using a numerical integration routine.

When evaluating the influence coefficients for M = N, i.e. the stresses at interval M due to unit body forces in the same interval, there is a singularity which must be taken into consideration when using numerical integration. The integrals either side of the singularity are evaluated in the normal manner and the integrand is approximated in the area of the singularity as follows:

$$F(\eta) = \frac{1}{\pi} \int_{y-\epsilon}^{y+\epsilon} \left[\frac{1}{(y-\eta)^2} - \frac{1}{(y+\eta)^2} + \frac{12y}{(y+\eta)^3} - \frac{12y^2}{(y+\eta)^4} \right] \sqrt{b^2 - (\eta-e)^2} \; d\eta$$

For small ϵ this becomes

$$F(\eta) \simeq \frac{1}{\pi} \int_{y-\epsilon}^{y+\epsilon} \frac{1}{(y-\eta)^2} \sqrt{b^2 - (\eta-e)^2} \; d\eta$$

Also for small ϵ, $\eta \simeq y$

$$\therefore \qquad F(\eta) \simeq \frac{1}{\pi} \sqrt{b^2 - (y-e)^2} \int_{y-\epsilon}^{y+\epsilon} \frac{1}{(y-\eta)^2} \; d\eta$$

$$= -\frac{2}{\pi\epsilon} \sqrt{b^2 - (y-e)^2}$$

Thus the total integral over an interval $[\eta_{N-1}, \eta_N]$ which contains a singularity can be evaluated numerically as the sum of three integrals over three sub-intervals, the outer two being performed using a standard numerical integration routine, while the middle one is a simple analytic expression.

3.1.6 Influence of Integration Parameters and Computer Precision

The influence coefficients which involved the singularities, $\sigma_{xM}^{\gamma M}$, were found to be affected by the choice of ϵ in the numerical integration. The error was linear with respect to ϵ, however, as shown in Table II, so extrapolation of the true value $\sigma_{xM}^{\gamma M}$ was straightforward.

The integration parameter ϵ was always calculated as a linear function of the fraction of the interval (FRAC) which is to be evaluated analytically around the singularity. In this way, as the intervals become smaller (as MM is increased) the value of ϵ shrinks accordingly without any change to FRAC.

TABLE II

INFLUENCE OF ϵ ON ERROR IN $\sigma_{x1}^{\gamma 1}$

FRAC	ϵ	ERROR IN $\sigma_{x1}^{\gamma 1}$
0.020	0.0020	0.00748
0.018	0.0018	0.00673
0.016	0.0016	0.00599
0.014	0.0014	0.00525
0.012	0.0012	0.00451
0.010	0.0010	0.00377
0.008	0.0008	0.00304
0.006	0.0006	0.00230
0.004	0.0004	0.00160
0.002	0.0002	0.00095

Results for crack in infinite plate in the interval [1.0, 1.2]
e = 2.0; b = 1.0; y = 1.1; MM = 10; ϵ = FRAC · b/MM

The correction factors F_{1A} and F_{1B} where

$$F_1 = \frac{K_1}{\sigma_x^\infty \sqrt{\pi b}}$$

and stress intensity factors were also found to vary linearly with respect to ϵ, so for a given MM, three or four values of ϵ were used in the numerical integration and the true values were extrapolated using linear regression.

The number of digits of precision specified for real program variables in the computer calculations was found to have a great effect on the results. For the NRC IBM 360 system, a 'single precision' real variable has six digits of precision, while a 'double precision' variable has fourteen. For these calculations it was necessary to specify double precision for all real variables.

The primary reason for this is that for small values of ϵ, several digits of precision are lost in the integration over intervals containing the singularities. When evaluating the integral over the three sub-intervals, the outer ones produced large positive numbers, while the centre produced a large negative number. When the three were added, the result was a number close to zero. Thus in the addition three or more digits of precision were lost.

3.1.7 Influence of Number of Intervals

Figure 7 shows that the error in the correction factor or stress intensity factor was linear with respect to 1/MM, and true values were therefore obtained by extrapolation to MM = ∞.

3.1.8 Results (Numerical Integration)

Table III compares the results obtained by numerical integration with those obtained analytically for various values of MM. The agreement is good and discrepancies can be attributed to approximation errors in the integration routine.

TABLE III

COMPARISON OF F_{1A} OBTAINED BY NUMERICAL AND ANALYTIC

INTEGRATIONS FOR CRACK IN SEMI-INFINITE PLATE

MM	FRAC			(EXTRAPOLATED)	ANALYTIC INTEGRATION
	0.03	0.02	0.01	0.00	
12	1.096155	1.094206	1.092265	1.090319	1.090367
16	1.096337	1.094411	1.092468	1.090536	1.090622
24	1.096515	1.094635	1.092756	1.090876	1.090919
32	1.096554	1.094688	1.092795	1.090920	1.091024
48	1.096608	1.094777	1.092938	1.091104	1.091243

$$b/e = 0.5 \qquad \epsilon = FRAC \cdot b/MM$$

The correction factor F_{1A} as ϵ tends to zero is plotted against $1/MM$ in Figure 7. Once again, the error in F_{1A} is nearly linear against $1/MM$ and the value tends to 1.091352 compared with a value of 1.091490 using analytic integration and 1.0914 obtained by Nisitani[1].

3.2 Edge Crack in a Semi-infinite Plate

3.2.1 Formulation

The case of a crack at the edge of a plate as in Figure 8 is similar to the case of an embedded crack. The edge of the plate is placed at the centre of the crack, so that the distance, e, from the edge to the centre of the crack is zero.

3.2.2 Results (Numerical Integration)

Table IV shows the correction factor F_{1B} for various values of the number of intervals, MM, and the integration parameter, FRAC, together with the extrapolated values for FRAC = 0.

The correction factor F_{1B} is plotted against $1/MM$ in Figure 9. The error in F_{1B} is almost linear in $1/MM$ with the value tending to 1.1213 as MM tends to infinity. This compares with a value of 1.121 given by Nisitani[1].

TABLE IV

COMPARISON OF F_{1B} FOR EDGE CRACK IN SEMI-INFINITE PLATE

AT VARIOUS VALUES OF MM

MM FRAC	F_{1B}			
	8	12	16	24
0.03	1.096820	1.098911	1.099955	1.101096
0.02	1.101942	1.104243	1.105375	1.106618
0.01	1.107365	1.109990	1.111269	1.112726
0.00 (EXTRAPOLATED)	1.112587	1.115460	1.116847	1.118443

$$\epsilon = FRAC \cdot b/2MM \quad ; \quad F_{1B} = \frac{K_{1B}}{\sigma_x^{\infty} \sqrt{\pi b}}$$

3.3 Elliptical Hole in an Infinite Plate

The numerical solution of problems involving holes is a little more complex than for cracks. It was therefore decided to first try the simple problem of an elliptical hole in an infinite plate since the body force densities are known and constant in this case, and this allows an intermediate check of the program.

3.3.1 Formulation

The elliptical hole shown in Figure 1 is divided into MM equal intervals and the body force densities, ρ_x and ρ_y are set constant within each interval. The influence coefficients are calculated from the stress field for a point force in an infinite plate and the boundary conditions that the mid-point of each interval be free from stress are applied to determine the body force densities. The stress concentration factors and the stresses at an arbitrary point on the plate can be found from a linear combination of the body force densities.

3.3.2 Solution Sequence

(1) The ellipse is divided into MM equal intervals, using the elliptic parameter φ used in the equations of an ellipse:

$$\xi = a \cos \varphi \quad ; \quad \eta = b \sin \varphi$$

The values of φ at the end points of the N-th interval are

$$\varphi_{N-1} = -\pi/2 + 2(N-1)\pi/MM$$

and
$$\varphi_N = -\pi/2 + 2N\pi/MM$$

The value of φ at the mid-point of the N-th interval is

$$\varphi = -\pi/2 + (2N-1)\pi/MM$$

The x and y values of the mid-point of the N-th interval are

$$x = a \cos (-\pi/2 + (2N-1)\pi/MM)$$

$$y = b \sin (-\pi/2 + (2N-1)\pi/MM)$$

(2) The influence coefficients, σ_{xM}^{XN}; σ_{xM}^{YN}; σ_{yM}^{XN}; σ_{yM}^{YN}; τ_{xyM}^{XN}; τ_{xyM}^{YN}, which are the stresses at the mid-point of the M-th interval due to a body force on the N-th interval having densities $\rho_x = 1$ or $\rho_y = 1$ are given in Appendix 3.

In the program listed in Reference 2, the influence coefficients for each point on the ellipse have been calculated. However, because of symmetry about the x and y axes the influence coefficients need only be calculated for one quarter of the ellipse, although for that quarter, all the influence coefficients must be calculated, i.e. the effects 'of body' forces around the total ellipse must be calculated.

(3) The boundary conditions to make the mid-point of each interval free from stresses are applied; i.e.

$$\sum_{N=1}^{MM} \rho_{xN} (\sigma_{xM}^{XN} \cos \theta + \tau_{xyM}^{XN} \sin \theta)$$

$$+ \sum_{N=1}^{MM} \rho_{yN} (\sigma_{xM}^{YN} \cos \theta + \tau_{xyM}^{YN} \sin \theta) + \sigma_{x}^{\infty} \cos \theta = 0$$

and

$$\sum_{N=1}^{MM} \rho_{xN} (\sigma_{yM}^{XN} \sin \theta + \tau_{xyM}^{XN} \cos \theta)$$

$$+ \sum_{N=1}^{MM} \rho_{yN} (\sigma_{yM}^{YN} \sin \theta + \tau_{xyM}^{YN} \cos \theta) = 0 \quad (M:1 \sim MM)$$

where ρ_{xN}, ρ_{yN} are the body force densities of the N-th interval, σ_{x}^{∞} is the stress at infinity and θ_M is the angle between the x axis and the normal to the ellipse at the mid-point of the M-th interval; i.e.

$$\theta_M = \arctan\left(\frac{a}{b}\tan\varphi_M\right)$$

where φ_M is the value of φ at the mid-point of the M-th interval.

This results in a system of 2MM linear equations in 2MM unknowns ρ_{xN}, ρ_{yN}.

(4) The stresses at any point P in the plate are calculated from the influence coefficients at that point and the body force densities; i.e.

$$\sigma_x = \sum_{N=1}^{MM}\left(\sigma_{xP}^{XN}\,\rho_{xN} + \sigma_{xP}^{YN}\,\rho_{yN}\right) + \sigma_x^\infty$$

$$\sigma_y = \sum_{N=1}^{MM}\left(\sigma_{yP}^{XN}\,\rho_{xN} + \sigma_{yP}^{YN}\,\rho_{yN}\right)$$

$$\tau_{xy} = \sum_{N=1}^{MM}\left(\tau_{xyP}^{XN}\,\rho_{xN} + \tau_{xyP}^{YN}\,\rho_{yN}\right)$$

(5) The stress concentration factors K_{TA}, K_{TB} are then calculated:

$$K_{TA} = \sigma_x\,(\text{at A})/\sigma_x^\infty$$

$$K_{TB} = \sigma_x\,(\text{at B})/\sigma_x^\infty$$

(6) Because the body force densities are constant around the ellipse, there will be no error due to the choice of the number of intervals MM. Therefore the value of the stress concentration factor will be the same regardless of the number of intervals.

3.3.3 Numerical Integration

In the numerical integration, the stress field equations have a singularity at $y = \eta$ and $x = \xi$, i.e. when the stresses are evaluated at the mid-point (x,y) of an interval due to a point force X or Y on the same interval. Integration is straightforward over all other intervals.

In order to integrate over the singularity, principal values of the integral are taken by splitting the integral in three disjoint subintervals

$$[\varphi_{N-1}, \varphi_{MID} - \epsilon];\ \ [\varphi_{MID} - \epsilon, \varphi_{MID} + \epsilon];\ \ [\varphi_{MID} + \epsilon, \varphi_N]$$

where $\qquad\qquad\qquad\qquad x = a\cos\varphi_{MID};\ y = b\sin\varphi_{MID}$

The integrals $F_1(\varphi)$ and $F_3(\varphi)$ over the 1st and 3rd subintervals are straightforward because the singularity occurs in F_2 over the 2nd subinterval.

If ϵ is small relative to the length of the interval $[\varphi_{N-1}, \varphi_N]$, $F_2(\varphi)$ can be approximated by a function which contains no singularity (see Appendix 4).

For this same M-th interval when $x = \xi$ and $y = \eta$, the stresses $\Delta\sigma_x^X$, $\Delta\sigma_x^Y$, $\Delta\sigma_y^X$, $\Delta\sigma_y^Y$, $\Delta\tau_{xy}^X$, $\Delta\tau_{xy}^Y$ which are the stresses at a point infinitesimally close to the ellipse subjected to a body force must be added to σ_{xM}^{XM}, σ_{xM}^{YM}, σ_{yM}^{XM}, σ_{yM}^{YM}, τ_{xyM}^{XM}, τ_{xyM}^{YM} respectively.

It can be shown (Appendix 5) that these additional stresses are

$$\Delta\sigma_x^X \bigg|_{\rho_X = 1} = -\frac{1}{16}(5 + 4\cos 2\theta - \cos 4\theta)$$

$$\Delta\sigma_y^X \bigg|_{\rho_X = 1} = \frac{1}{16}(1 - \cos 4\theta)$$

$$\Delta\tau_{xy}^X \bigg|_{\rho_X = 1} = -\frac{1}{16}(2\sin 2\theta - \sin 4\theta)$$

and

$$\Delta\sigma_x^Y \bigg|_{\rho_y = 1} = \frac{1}{16}(1 - \cos 4\theta)$$

$$\Delta\sigma_y^Y \bigg|_{\rho_y = 1} = -\frac{1}{16}(5 - 4\cos 2\theta - \cos 4\theta)$$

$$\Delta\tau_{xy}^Y \bigg|_{\rho_y = 1} = -\frac{1}{16}(2\sin 2\theta + \sin 4\theta)$$

where θ is the angle between the x axis and the normal to the ellipse at the mid-point of the M-th interval.

3.3.4 Results

Table V shows the body force densities ρ_x and ρ_y for each interval of a circular ellipse in an infinite plate.

The results are identical to those predicted by the theory in Section 2.1. The body force densities are constant around the ellipse and agree with equations

$$\rho_x = \sigma_x^\infty(1 + 2b/a) = 3\sigma_x^\infty = 3$$

$$\rho_y = -\sigma_x^\infty = -1$$

TABLE V

BODY FORCE DENSITIES FOR CIRCLE IN INFINITE PLATE

Interval	ρ_x	ρ_y
1	3.000000	-1.000000
2	3.000000	-1.000000
3	3.000000	-1.000000
4	3.000000	-1.000000
5	3.000000	-1.000000
6	3.000000	-1.000000
7	3.000000	-1.000000
8	3.000000	-1.000000

MM = 8; FRAC = 0.02; ϵ = FRAC $\cdot$ π/MM
a = 1.0; b = 1.0; σ_x^∞ = 1.0

3.4 Elliptic and Semi-elliptic Hole in a Semi-infinite Plate

3.4.1 Formulation

For the case of an ellipse or a semi-ellipse in a semi-infinite plate, Figure 10, the densities of body force ρ_x and ρ_y are no longer constant as in the case of the ellipse in an infinite plate. Instead the densities are continuously varying around the edge of the hole.

If the elliptic hole is partitioned into MM intervals and ρ_x, ρ_y are set constant within each interval, the continuously varying densities will be replaced by a stepped distribution which will be accurate for large values of MM.

The stress field due to a point force in a semi-infinite plate is used to evaluate the stresses at the mid-point of each interval. The boundary conditions that the mid-point of each interval be free from stresses are applied and the values of the body force densities can then be evaluated.

The stresses at an arbitrary point in the plate and the stress concentration factor (SCF) at the top or bottom of the semi-ellipse or ellipse can be calculated by taking a linear combination of the body force densities.

Due to the symmetry of the ellipse or semi-ellipse about the y-axis, only half of the influence coefficients need to be calculated although, as before, they must be evaluated for body forces around the total ellipse.

3.4.2 Solution Sequence

(1) The ellipse or semi-ellipse in a semi-infinite plate is divided into MM intervals. For the ellipse, the values of the elliptic parameter φ at the end points of the N-th interval are

$$\varphi_{N-1} = -\pi/2 + 2(N-1)\pi/MM$$

$$\varphi_N = -\pi/2 + 2N\pi/MM$$

The x and y values of the mid-point of the N-th interval are

$$x = a \cos(-\pi/2 + (2N-1)\pi/MM)$$

$$y = b \sin(-\pi/2 + (2N-1)\pi/MM)$$

For the semi-ellipse, the values of φ at the end points of the N-th interval are

$$\varphi_{N-1} = (N-1)\pi/MM$$

$$\varphi_N = N\pi/MM$$

The x and y values of the mid-point of the N-th interval are

$$x = a \cos((N-0.5)\pi/MM)$$

$$y = b \sin((N-0.5)\pi/MM)$$

(2) The influence coefficients σ_{xM}^{XN}, σ_{xM}^{YN}, σ_{yM}^{XN}, σ_{yM}^{YN}, τ_{xyM}^{XN}, τ_{xyM}^{YN}, which are the stresses at the mid-point of the M-th interval due to a body force on the N-th interval Y in a semi-infinite plate having density $\rho_x = 1$ or $\rho_y = 1$ are given in Appendix 3.

(3) The remainder of the solution sequence is identical to that for an ellipse in an infinite plate.

3.4.3 Influence of the Integration Parameter

The method of numerical integration is identical to that for an ellipse in an infinite plate. However, for a semi-infinite plate the influence coefficients which involve singularities and hence the stress concentration factors are affected by the choice of the value of ϵ in the numerical integrations.

Table VI shows the stress concentration factors obtained for various values of the integration parameter ϵ for a semi-ellipse with $b/a = 2.0$ in a semi-infinite plate.

TABLE VI

EFFECT OF ϵ ON SCF FOR SEMI-ELLIPSE

IN SEMI-INFINITE PLATE

FRAC	SCF
0.010	5.187062
0.008	5.185324
0.005	5.182725
0.001	5.179275
extrapolated to 0	5.1784

MM = 16; a = 1, b = 2, e = 0, ϵ = FRAC $\cdot \pi/MM$

In Figure 11 the SCF is plotted against ϵ. The error in the SCF is almost linear in ϵ, and tends to 5.1784 as ϵ tends to zero.

Because of the linearity of the error in the SCF, it is only necessary to obtain two or three values of the SCF for different values of ϵ and extrapolate to obtain the value of SCF for $\epsilon = 0$. Another method of approximating the true SCF for a given number of cuts is to choose ϵ_0 small enough that the difference between the value of the SCF at $\epsilon = 0$ and the value at ϵ_0 is negligible.

3.4.4 Results

Tables VII and VIII compare the results obtained for a semicircular notch, and an ellipse with b/a = 2.0 and e = 0.5, with those of Nisitani[1,4] for several values of the number of intervals MM. The agreement is excellent. Discrepancies can be explained by the fact that the integration parameter ϵ is taken to be very small, but no extrapolation has been done to determine the true value at $\epsilon = 0$. This was done to reduce the amount of computer time used.

TABLE VII

STRESS CONCENTRATION FACTORS FOR A

SEMICIRCLE IN A SEMI-INFINITE PLATE

MM \ K_{TB}	Present Results	Nisitani[4]
16	3.053872	3.0527
24	3.057044	3.05595
32	3.059274	3.05908
48	3.061416	3.06123

a = 1; b = 1; FRAC = 0.001

TABLE VIII

STRESS CONCENTRATION FACTORS FOR AN

ELLIPSE IN A SEMI-INFINITE PLATE

MM \ K_{TA}	Present Results	Nisitani[1]
16	5.696703	—
24	5.715367	5.7147
32	5.724825	5.7243
48	5.734337	5.7340

a = 1; b = 2; e = 0.5; FRAC = 0.001

Figures 12 and 13 show K_{TA} and K_{TB} as a function of 1/MM. The error in the K_T's is almost linear in 1/MM. For the semicircle on the edge of the plate, K_{TB} tends to 3.0650 as MM tends to infinity, compared with a value of 3.0654 obtained by Nisitani[4] and 3.0653 by Isida[5]. For the ellipse (b/a = 2.0, e = 0.5) K_{TA} tends to 5.7531 as MM tends to ∞, compared with a value of 5.753 obtained by Nisitani.

3.5 Combination of a Crack and an Elliptical Hole in a Semi-infinite Plate

3.5.1 Formulation

Figure 14 shows the case of a crack and an elliptic edge notch in a semi-infinite plate. As before, the semi-ellipse is divided into M1 equal intervals and the crack into M2 equal intervals, with the body force densities set constant within each interval. The stress field due to a point force in a semi-infinite plate and its derivatives are used to calculate the stresses at the mid-point of each interval on both the crack and the semi-ellipse due to the body forces on both, and the conditions to make the mid-point of each interval free of stress are applied. The body force densities can then be determined as before.

3.5.2 Solution Sequence

(1) The semi-ellipse is divided into M1 equal intervals. The end points of the N-th interval have φ values

$$\varphi_{N-1} = (N-1)\pi/M1$$

$$\varphi_N = N\pi/M1$$

where φ is the elliptic parameter such that

$$\xi = a\cos\varphi; \qquad \eta = b\sin\varphi$$

The x and y values of the mid-point of the M-th interval are

$$x = a\cos((M-0.5)\pi/M1)$$

$$y = b\sin((M-0.5)\pi/M1)$$

The crack is divided into M2 equal intervals. The end points of the N-th interval have values on the y axis

$$\eta_{N-1} = e - c + 2(N-1)c/M2$$

$$\eta_N = e - c + 2Nc/M2$$

where e is the distance from the edge of the plate to the centre of the crack, and c is half the length of the crack.

The mid-point of the M-th interval has a value

$$y = e - c + (2M - 1) c/M2$$

(2) The influence coefficients

$$\sigma_{xMe}^{XN}, \; \sigma_{yMe}^{XN}, \; \sigma_{xMe}^{YN}, \; \sigma_{yMe}^{YN}, \; \tau_{xyMe}^{XN}, \; \tau_{xyMe}^{YN}$$

$$\sigma_{xMe}^{\gamma N}, \; \sigma_{yMe}^{\gamma N}, \; \tau_{xyMe}^{\gamma N}$$

$$\sigma_{xMc}^{XN}, \; \sigma_{xMc}^{YN}$$

and
$$\sigma_{xMc}^{\gamma N}$$

are given in the appendices.

The first six coefficients are the stresses at the mid-point of the M-th interval on the ellipse due to point forces on the N-th interval of the ellipse having densities $\rho_x = 1$ or $\rho_y = 1$ (see Appendix 3).

The seventh to ninth coefficients are the stresses at the mid-point of the M-th interval on the ellipse due to a pair of point forces in the N-th interval of the crack having density $\gamma = 1$ (see Appendix 6).

The 10th and 11th coefficients are the stresses at the mid-point of the M-th interval on the crack due to point forces on the N-th interval of the ellipse (see Appendices 3 and 6).

The 12th coefficient is the stress at the mid-point of the M-th interval on the crack due to a pair of point forces on the N-th interval of the crack (see Appendix 2).

(3) The boundary conditions that the mid-point of each interval on the ellipse and crack be free from stress are applied:

$$\sum_{N=1}^{M1} \left[\rho_{xN} \left(\sigma_{xMe}^{XN} \cos \theta + \tau_{xyMe}^{XN} \sin \theta \right) + \rho_{yN} \left(\sigma_{xMe}^{YN} \cos \theta + \tau_{xyMe}^{YN} \sin \theta \right) \right]$$

$$+ \sum_{N=1}^{M2} \gamma_N \left(\sigma_{xMe}^{\gamma N} \cos \theta + \tau_{xyMe}^{\gamma N} \sin \theta \right) + \sigma_x^{\infty} \cos \theta = 0$$

$$\sum_{N=1}^{M1} \left[\rho_{xN} \left(\sigma_{yMe}^{XN} \sin \theta + \tau_{xyMe}^{XN} \cos \theta \right) + \rho_{yN} \left(\sigma_{yMe}^{YN} \sin \theta + \tau_{xyMe}^{YN} \cos \theta \right) \right]$$

$$+ \sum_{N=1}^{M2} \gamma_N \left(\sigma_{yMe}^{\gamma N} \sin \theta + \tau_{xyMe}^{\gamma N} \cos \theta \right) = 0$$

$$\sum_{N=1}^{M1} \left[\rho_{xN} \sigma_{xMc}^{XN} + \rho_{yN} \sigma_{xMc}^{YN} \right] + \sum_{N=1}^{M2} \gamma_N \sigma_{xMc}^{\gamma N} + \sigma_x^{\infty} = 0$$

The result is a system of (2M1 + M2) linear equations in (2M1 + M2) unknowns ρ_x, ρ_y and γ.

3.5.3 Numerical Integration

In the numerical integration of the influence coefficients, singularities occurred in the evaluation of the first six coefficients discussed in 3.5.2, and in the 12th. The procedure for handling the first six coefficients is discussed in 3.3.3, while the procedure for the 12th coefficient is discussed in 3.1.5. However, it is not necessary to evaluate the 12th coefficient numerically. As seen in 3.1.3 (for a crack of length 2c) or 3.2.1 (for a crack at the edge of a semi-ellipse) the 12th coefficient can be evaluated analytically.

3.5.4 Results

The values of the correction factors at both tips of a crack in a semi-infinite plate having a semi-elliptical notch are given for various values of the number of intervals M1 and M2 in Table IX.

TABLE IX

CORRECTION FACTORS FOR A CRACK NEXT TO A

SEMI-ELLIPTICAL NOTCH IN SEMI-INFINITE PLATE

No. of Intervals		Correction Factors	
M1	M2	F_{IA}	F_{IB}
16	16	2.201207	1.935246
24	24	2.211444	1.938788
32	32	2.217546	1.940605
48	48	2.222124	1.941886

c = 100.0; ρ = 1000.0; c/ρ = 0.1
a = 1000.0; b = 1000.0; b/a = 1.0
c/h = 0.4; FRAC = 0.05; ϵ = FRAC · π/MM

The correction factors are plotted against $1/(M1 + M2)$ in Figure 15 and again the error is almost linear in $1/(M1 + M2)$. The extrapolated values as $M1 + M2$ tend to infinity are 2.2329 for F_{1A} and 1.9454 for F_{1B} compared with the values of 2.232 and 1.944 obtained by Nisitani[11].

4.0 SUMMARY AND CONCLUSIONS

An outline of Nisitani's body force method has been presented and several problems have been solved using the technique. The problems include single embedded cracks and edge cracks and single elliptical and semi-elliptical notches in semi-infinite plates, as well as the problem of an embedded crack near a semi-elliptical notch in a semi-infinite plate. Results agree very well with those of Nisitani and solution times are relatively short.

Details of the numerical technique have been presented, including a brief discussion of the computer precision required and the method for integrating over the singularities. In addition, all the analytical details for each problem have been presented, gathering together information from several of Nisitani's papers, many of which are in Japanese.

Full details of the computer programs are provided in a separate report.

5.0 ACKNOWLEDGEMENTS

6.0 REFERENCES

1. Nisitani, H.   *Solutions of Notch Problems by Body Force Method.*
                          Mechanics of Fracture, Vol. 5, ed. G.C. Sih, Sijthoff and Noordhoff,
                          The Netherlands, 1978.

2. Fraga, W.E.   *Computer Programs for Solving Notch Problems using Nisitani's Body
    Hewitt, R.L.   Force Method.*
                          NRC Laboratory Technical Report LTR-ST-1479, National Research
                          Council Canada, November 1983.

3. Timoshenko, S.P.   *Theory of Elasticity.*
    Goodier, J.N.   McGraw-Hill Book Company, New York, 1951.

4. Nisitani, H.   *The Two-Dimensional Stress Problem Solved using an Electric Digital
                          Computer.*
                          Bulletin of JSME, Vol. 11, No. 43, pp. 14-23, 1968.

5. Isida, M.   *Stress Intensity Factors for the Tension of an Eccentrically Cracked
                          Strip.*
                          J. App. Mech, Vol. 33, pp. 674-675, 1966.

6. Nisitani, H.   *Tension of a Semi-infinite Plate with a Row of Elliptic Holes (including
    Suematsu, M.   cracks) or an Infinite Plate with Two Rows of Elliptic Holes.*
    Saito, K.   Transactions of the Japan Society of Mechanical Engineers, Vol. 39,
                          No. 324, pp. 2323-2330, 1973 (in Japanese).

7. Nisitani, H.   *Stress Concentration Due to an Elliptic Hole or Crack Existing near a
    Saito, K.   Notch Under Tension or Longitudinal Shear.*
    Hara, N.   Transactions of the Japan Society of Mechanical Engineers, Vol. 39,
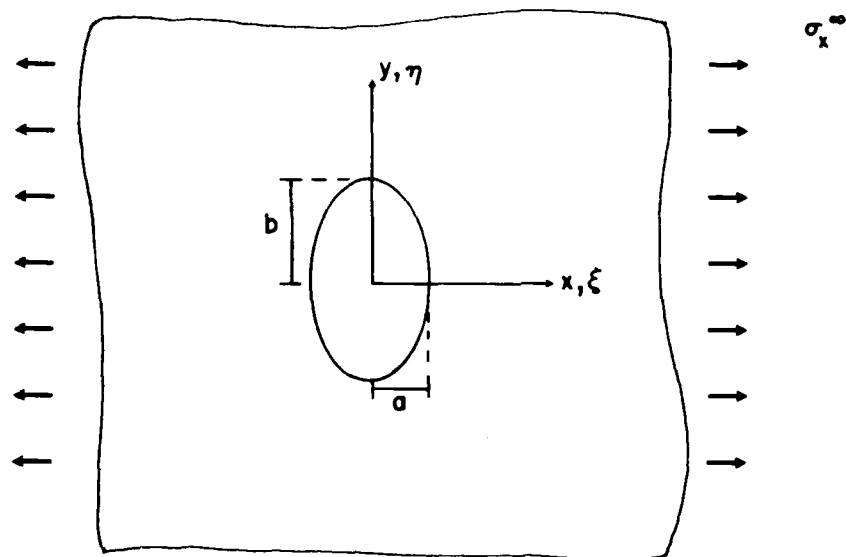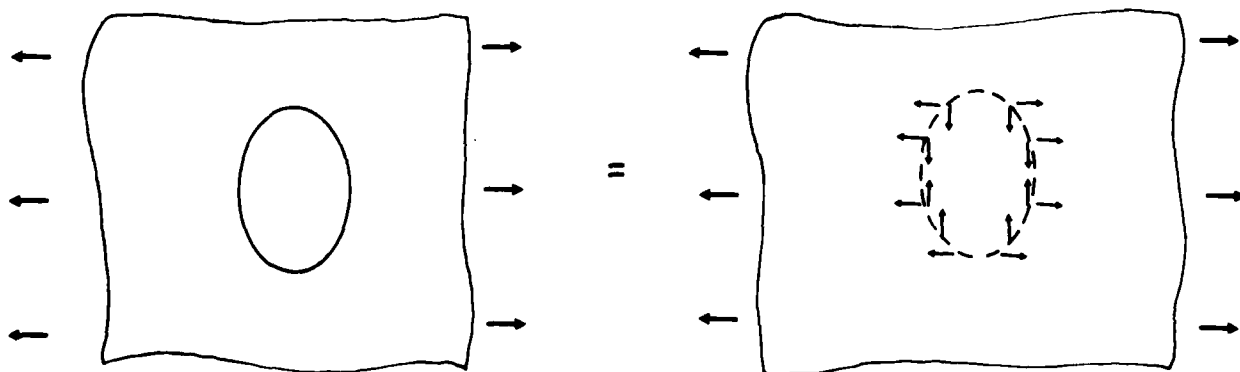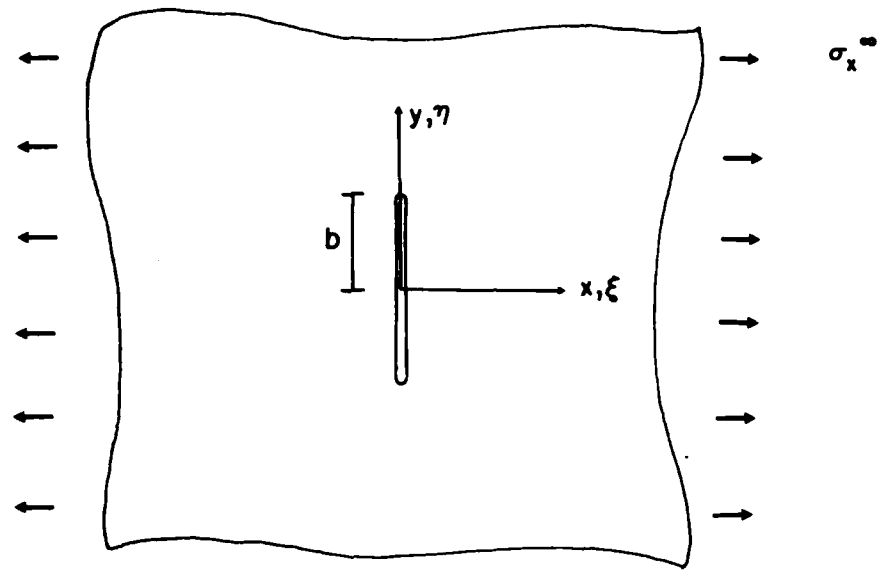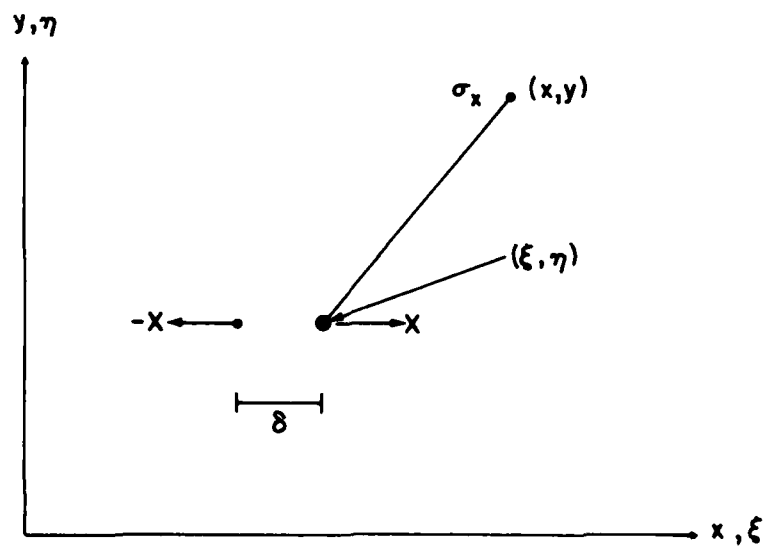   No. 324, pp. 2312-2322, 1973 (in Japanese).

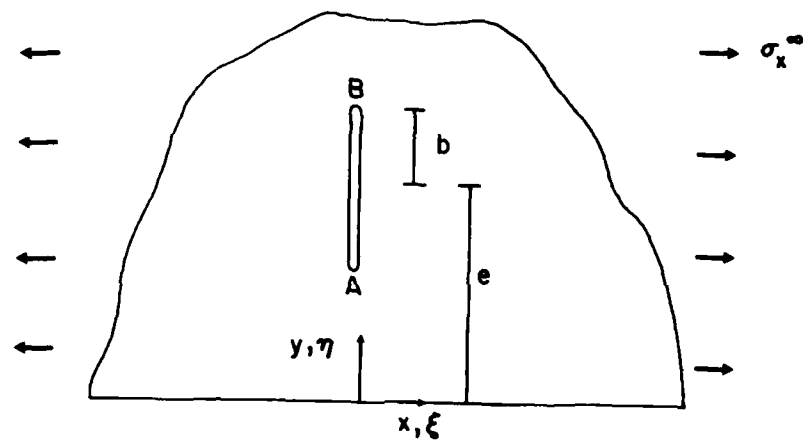**FIG. 1**
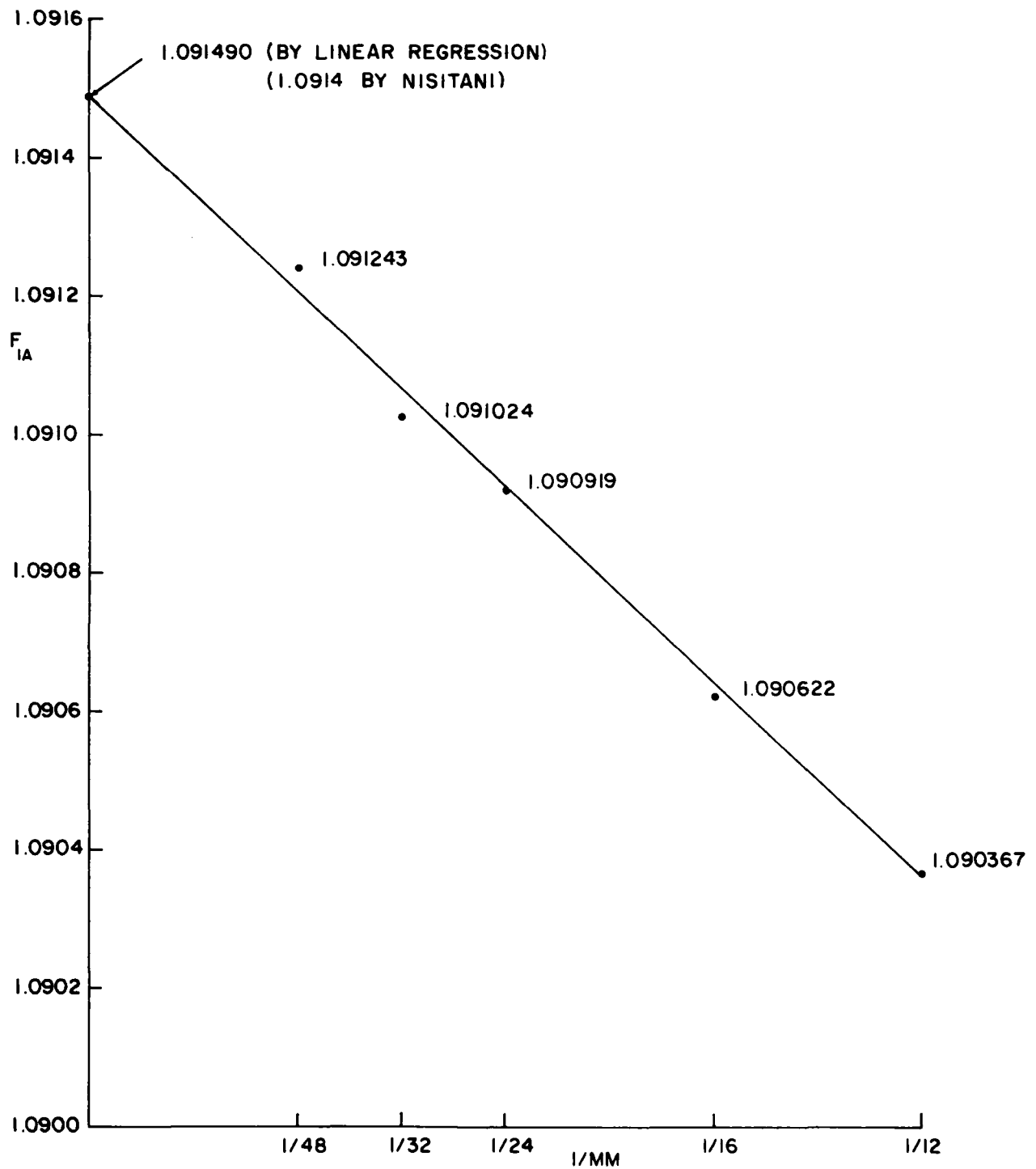

FIG. 2

FIG. 3

FIG. 4

FIG. 5

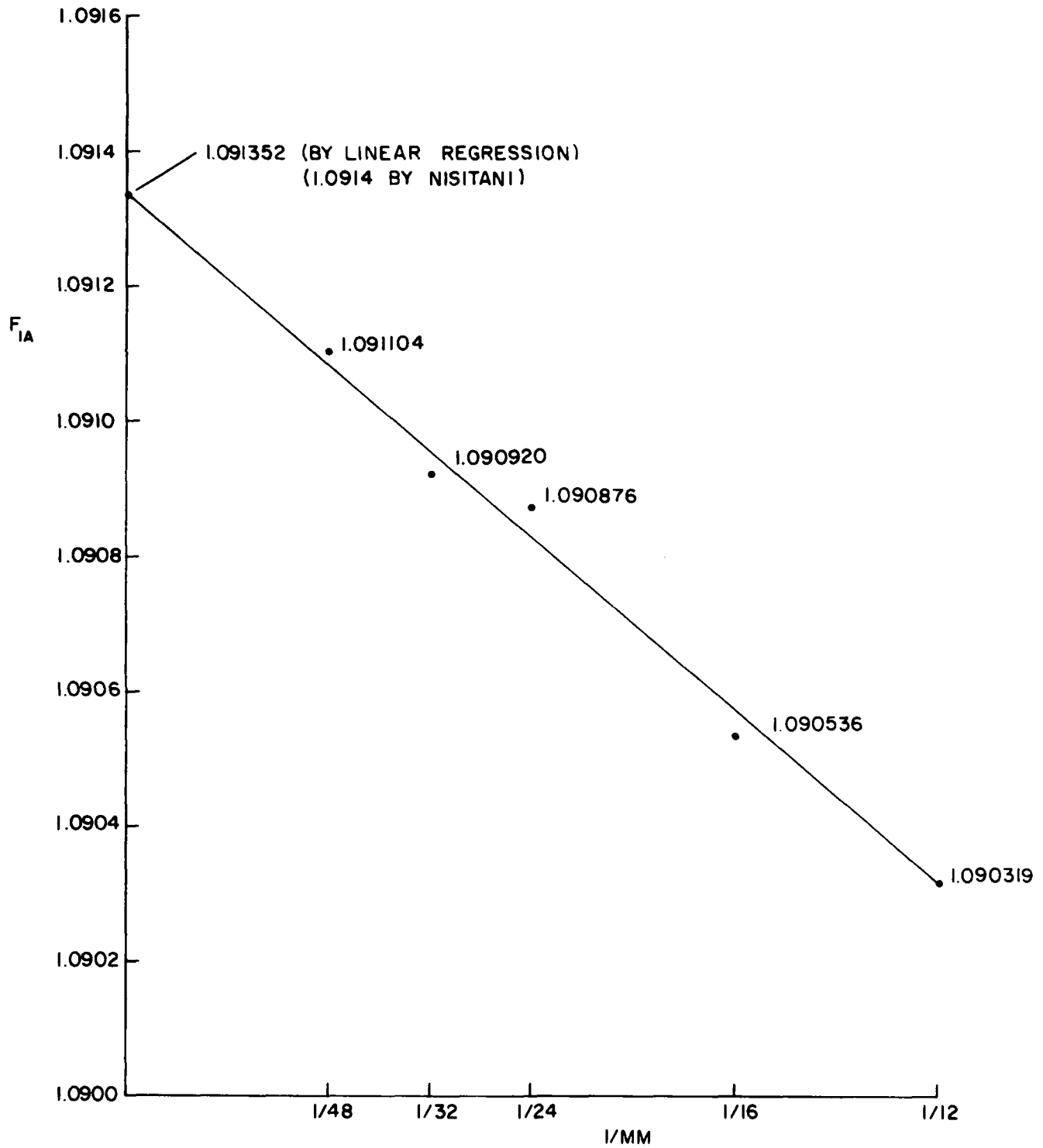**FIG. 6: CRACK IN SEMI-INFINITE PLATE**
(b/e = 0.5, ANALYTIC INTEGRATION)

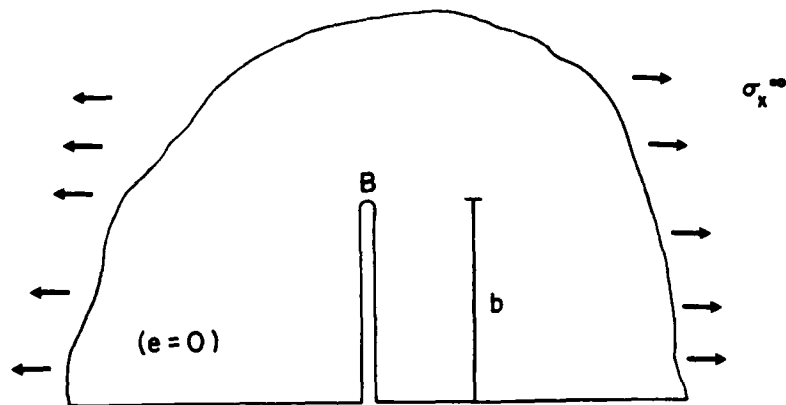FIG. 7: CRACK IN SEMI-INFINITE PLATE
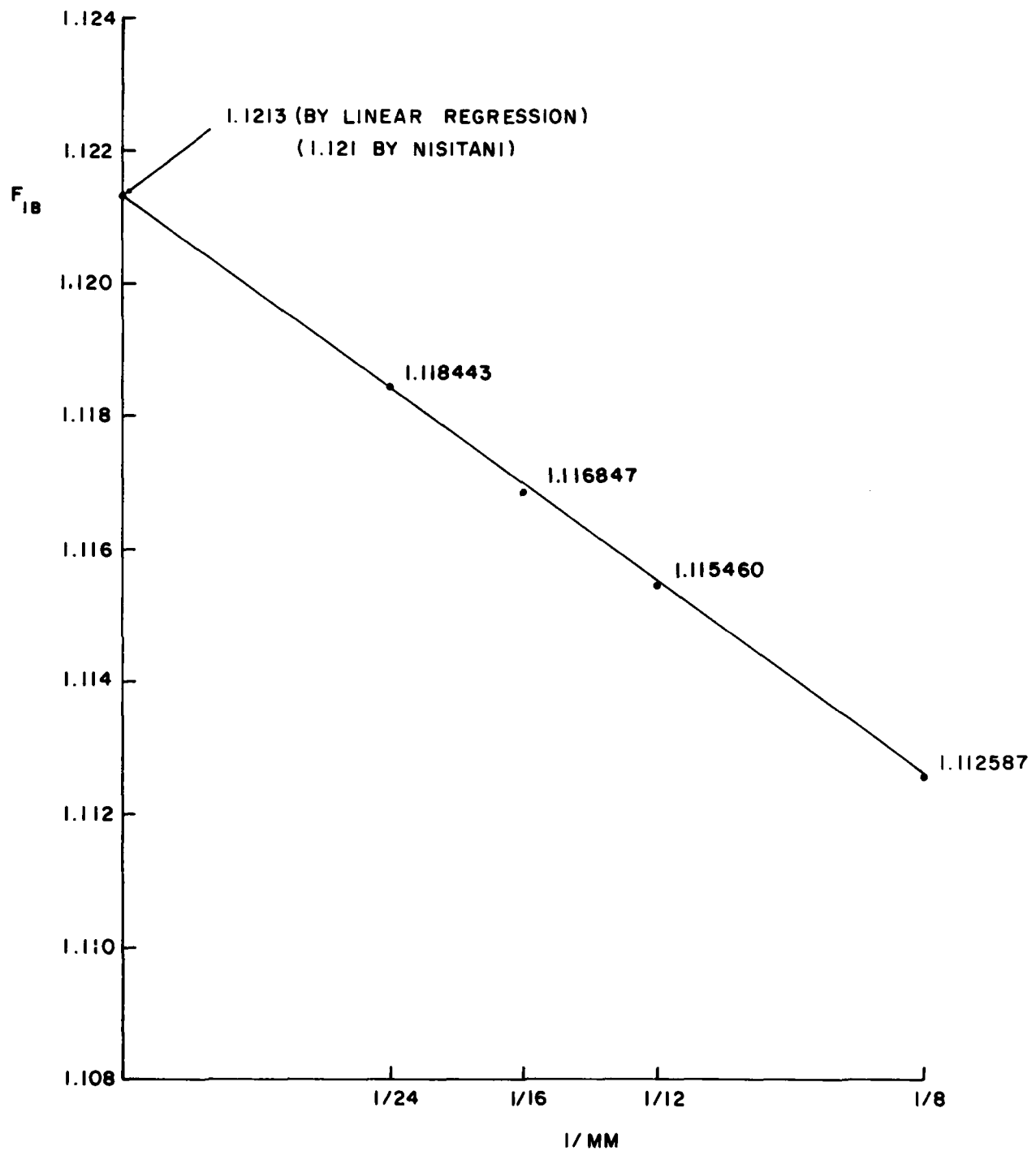(b/e = 0.5, NUMERICAL INTEGRATION)

FIG. 8
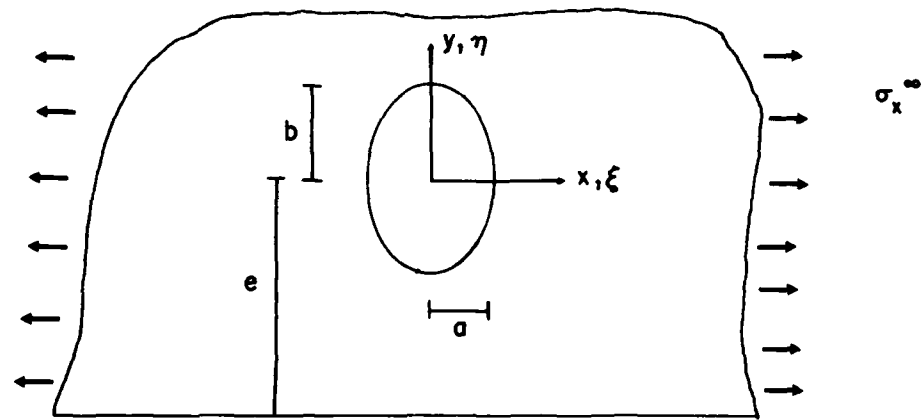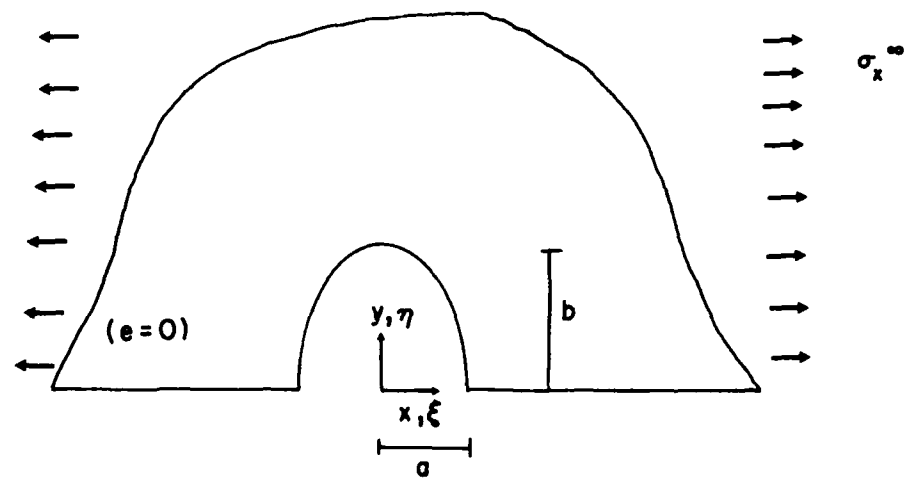
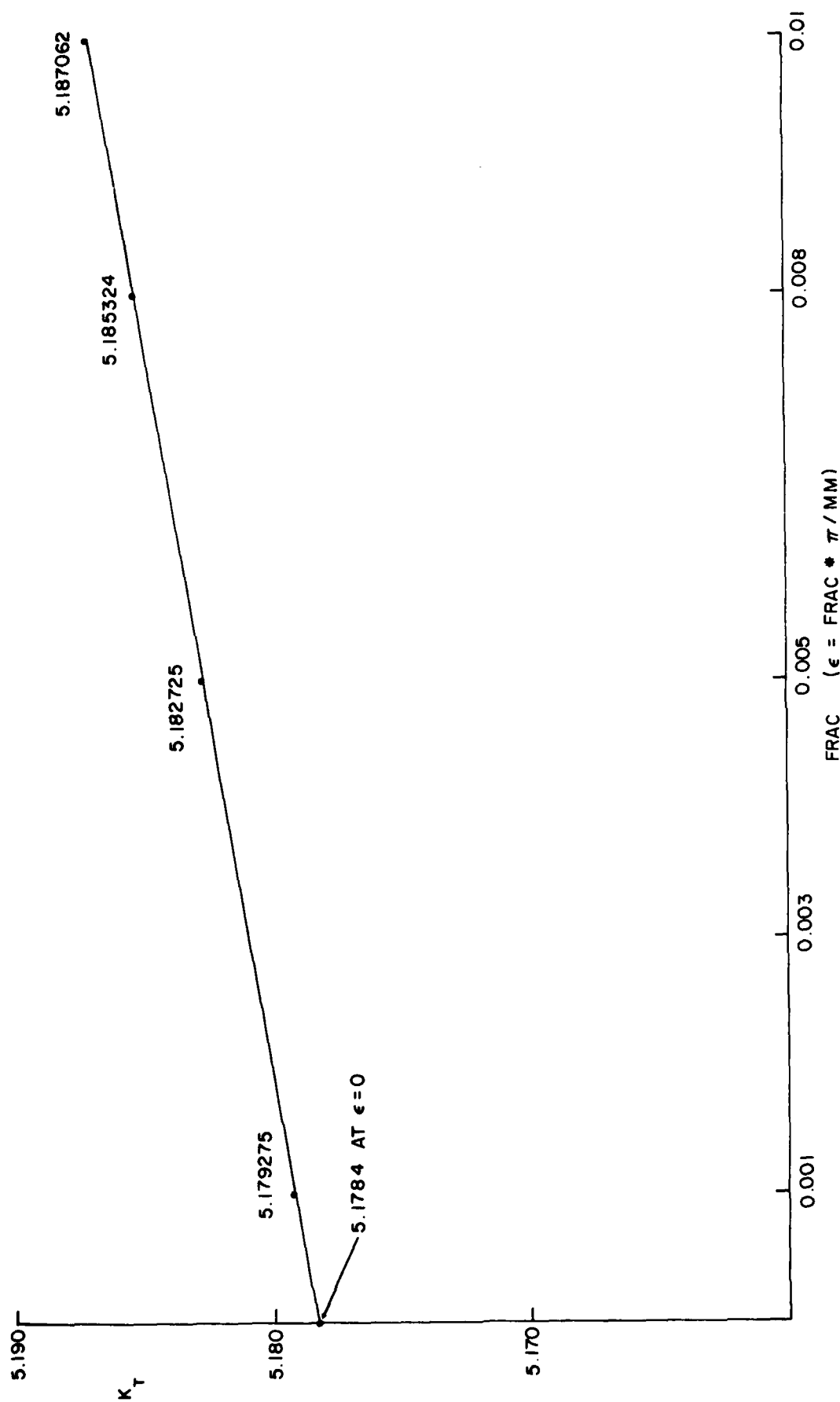FIG. 9: EDGE CRACK IN SEMI-INFINITE PLATE
(e = 0.0)

(a)

(b)

FIG. 10

FIG. 11: EFFECT OF EPSILON FOR SEMI-ELLIPSE IN SEMI-INFINITE PLATE
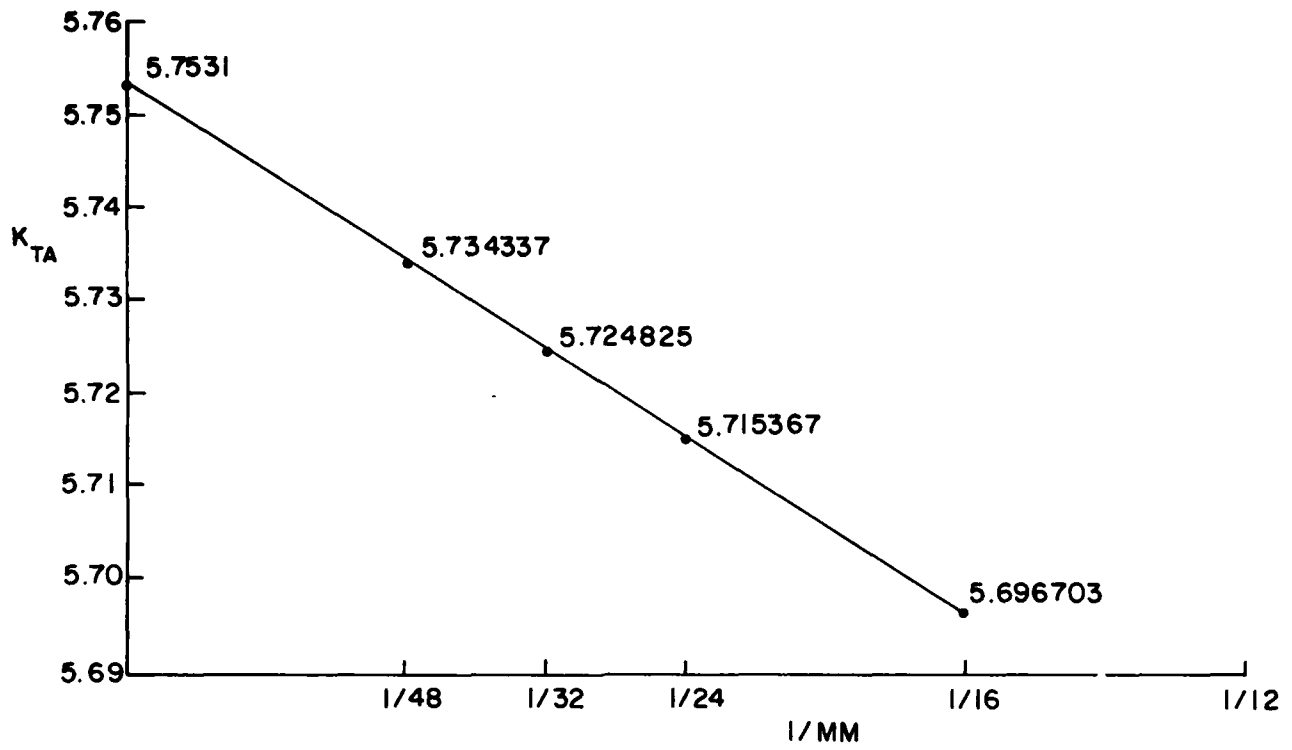(b/a = 2.0, ε = 0.0, MM = 16)

FIG. 12: ELLIPSE IN SEMI-INFINITE PLATE
(b/a = 2.0, e = 4.0, FRAC = 0.001)

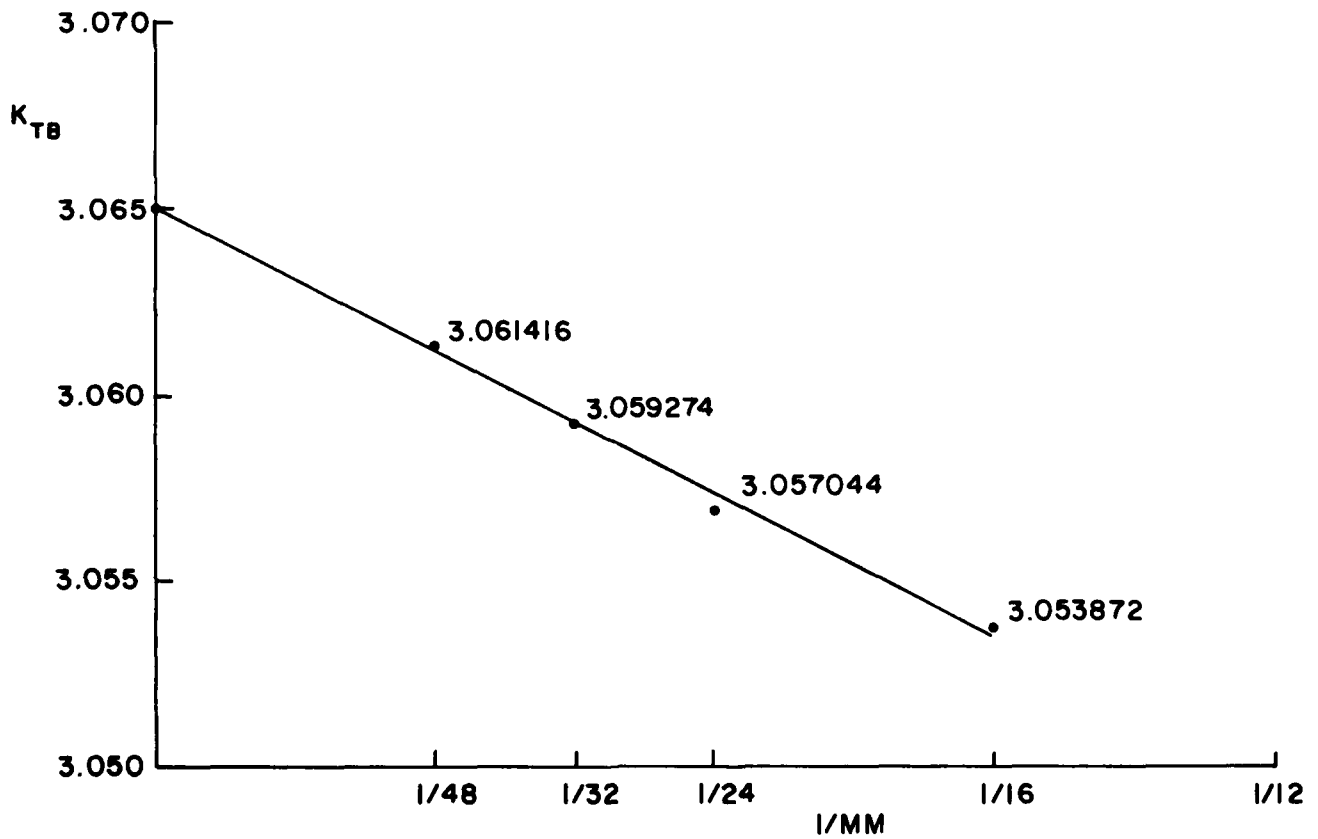**FIG. 13: SEMI-ELLIPSE IN SEMI-INFINITE PLATE**
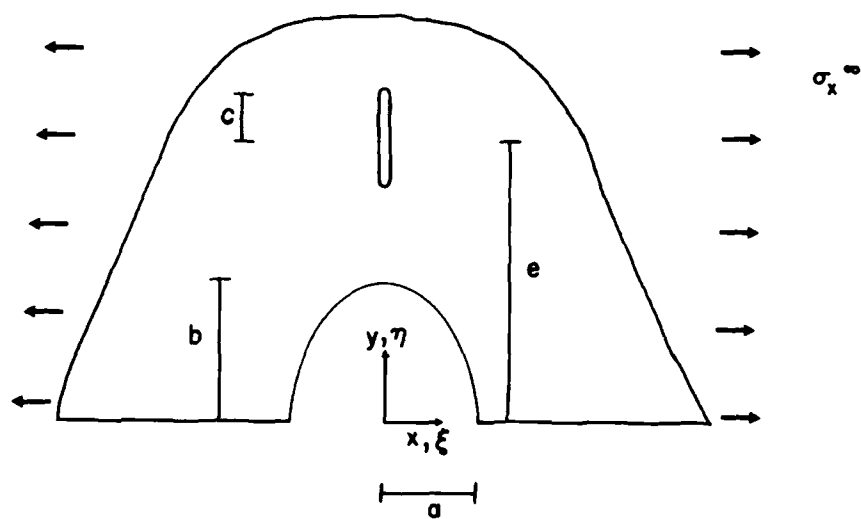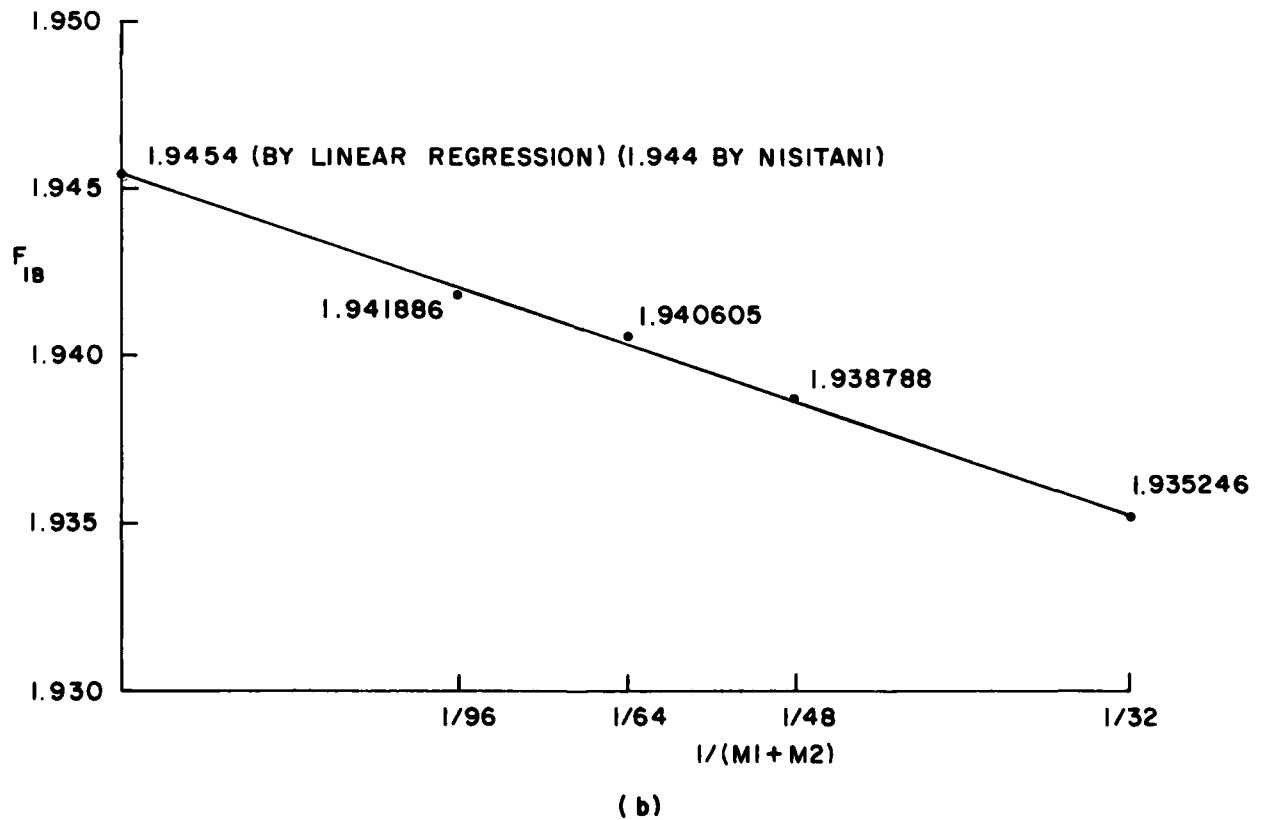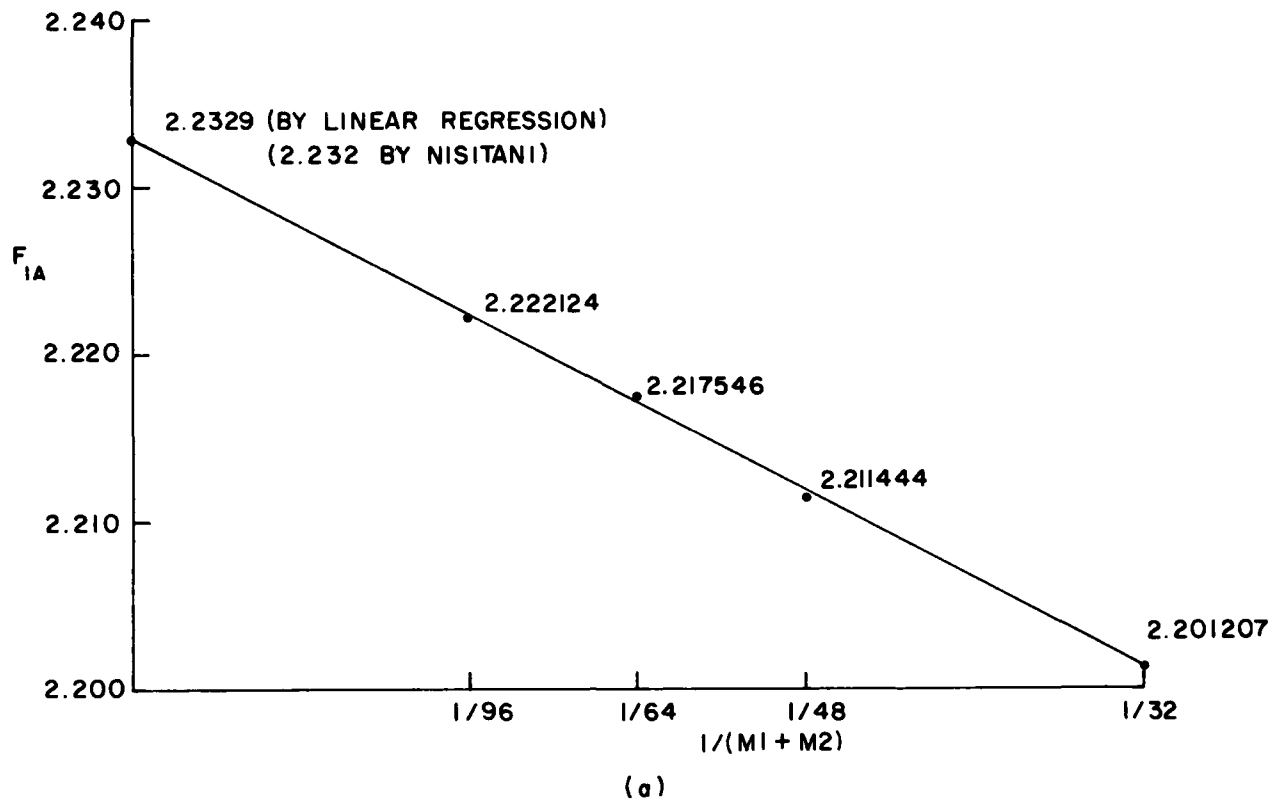(b/a = 1.0, e = 0, FRAC = 0.001)

FIG. 14

FIG. 15: ELLIPSE AND CRACK IN SEMI-INFINITE PLATE
(c/h = 0.4, FRAC = 0.05)

APPENDIX 1: FUNDAMENTAL STRESS FIELDS

For plane stress, the stress fields at (x,y) for point forces X and Y acting at (ξ, η) are[1]:

$$\sigma_x^X = -F\ell \left\{ (3 + \nu)\ell^2 + (1 - \nu)m^2 \right\} X$$

$$\sigma_y^X = F\ell \left\{ (1 - \nu)\ell^2 - (1 + 3\nu)m^2 \right\} X$$

$$\tau_{xy}^X = -Fm \left\{ (3 + \nu)\ell^2 + (1 - \nu)m^2 \right\} X$$

and

$$\sigma_x^Y = -Fm \left\{ (1 + 3\nu)\ell^2 - (1 - \nu)m^2 \right\} Y$$

$$\sigma_y^Y = -Fm \left\{ (1 - \nu)\ell^2 + (3 + \nu)m^2 \right\} Y$$

$$\tau_{xy}^Y = -F\ell \left\{ (1 - \nu)\ell^2 + (3 + \nu)m^2 \right\} Y$$

for an infinite plate, and

$$\sigma_x^X = \left[-F\ell \left\{ (3 + \nu)\ell^2 + (1 - \nu)m^2 \right\} - G_1 \ell \left\{ (3 + \nu)\ell^2 + (1 - \nu)n^2 \right\} \right.$$

$$- G_2 \left\{ (1 - \nu)(\ell^5 + 2(n^2 - n)\ell^3 + n^2(n^2 - 2n)\ell) \right.$$

$$\left. + (1 + \nu)(-2(n^2 - 1)\ell^3 + n^2(-2n^2 + 8n - 6)\ell) \right\} \right] X$$

$$\sigma_y^X = \left[F\ell \left\{ (1 - \nu)\ell^2 - (1 + 3\nu)m^2 \right\} + G_1 \ell \left\{ (1 - \nu)\ell^2 - (1 + 3\nu)n^2 \right\} \right.$$

$$- G_2 \left\{ (1 - \nu)(\ell^5 + 2(n^2 + n)\ell^3 + n^2(n^2 + 2n)\ell) \right.$$

$$\left. + (1 + \nu)(2(-n^2 + 2n - 1)\ell^3 + n^2(-2n^2 - 4n + 6)\ell) \right\} \right] X$$

$$\tau_{xy}^X = \left[-Fm \left\{ (3 + \nu)\ell^2 + (1 - \nu)m^2 \right\} - G_1 n \left\{ (3 + \nu)\ell^2 + (1 - \nu)n^2 \right\} \right.$$

$$\left. + G_2 \left\{ (1 - \nu)(-\ell^4 + n^4) + (1 + \nu)(6n(n - 1)\ell^2 + n^3(-2n + 2)) \right\} \right] X$$

and

$$\sigma_x^Y = \left[-\, Fm \left\{ (1 + 3\nu)\ell^2 - (1 - \nu)m^2 \right\} + G_1 n \left\{ (1 + 3\nu)\ell^2 - (1 - \nu)n^2 \right\} \right.$$

$$- G_2 \left\{ (1 - \nu)((n + 1)\ell^4 + 2n^3\ell^2 + n^3(n^2 - n)) \right.$$

$$\left. \left. + (1 + \nu)(2\ell^4 + n(2n^2 + 6n - 6)\ell^2 + n^3(2n^2 - 4n + 2)) \right\} \right] Y$$

$$\sigma_y^Y = \left[-\, Fm \left\{ (1 - \nu)\ell^2 + (3 + \nu)m^2 \right\} + G_1 n \left\{ (1 - \nu)\ell^2 + (3 + \nu)n^2 \right\} \right.$$

$$- G_2 \left\{ (1 - \nu)((n - 1)\ell^4 + 2n^3\ell^2 + n^3(n^2 + n)) \right.$$

$$\left. \left. + (1 + \nu)(n(2n^2 - 6n + 6)\ell^2 + n^3(2n^2 + 2n - 2)) \right\} \right] Y$$

$$\tau_{xy}^Y = \left[-\, F\ell \left\{ (1 - \nu)\ell^2 + (3 + \nu)m^2 \right\} + G_1 \ell \left\{ (1 - \nu)\ell^2 + (3 + \nu)n^2 \right\} \right.$$

$$\left. - G_2 \left\{ (1 - \nu)(2n\ell^3 + 2n^3\ell) + (1 + \nu)(2\ell^3 + n^2(8n - 6)\ell) \right\} \right] Y$$

for a semi-infinite plate, where

$$\ell = \frac{x - \xi}{y}, \qquad m = \frac{y - \eta}{y}, \qquad n = \frac{y + \eta}{y}$$

$$F = \frac{1}{4\pi y\,(\ell^2 + m^2)^2}, \qquad G_1 = \frac{1}{4\pi y\,(\ell^2 + n^2)^2}, \qquad G_2 = \frac{1}{2\pi y\,(\ell^2 + n^2)^3}$$

APPENDIX 2: ANALYTIC INTEGRATION FOR CRACK IN SEMI-INFINITE PLATE

Stress at the M-th interval due to a pair of point forces at the N-th interval on a crack:

$$\sigma_{xM}^{\gamma N} = \int_N \left. \frac{\partial \sigma_x^X}{\partial \xi} \right|_{\substack{X=1 \\ x=\xi=0}} \left\{ 4\gamma_N \sqrt{b^2 - (\eta - e)^2} \right\} \bigg|_{\gamma_N = 1} d\eta$$

$$= \int_{\eta_{N-1}}^{\eta_N} \left[\frac{1}{4\pi (y - \eta)^2} + \frac{1}{4\pi} \left\{ -\frac{1}{(y + \eta)^2} + \frac{12y}{(y + \eta)^3} - \frac{12y^2}{(y + \eta)^4} \right\} \right]$$

$$\times \left\{ 4 \sqrt{b^2 - (\eta - e)^2} \right\} d\eta$$

where η_{N-1} and η_N denote the values of η at both ends of the N-th interval. The integral can be obtained in closed form as follows[1]:

$$\sigma_{xM}^{\gamma N} = F(\eta_N) - F(\eta_{N-1})$$

in which $F(\eta)$ stands for

$$F(\eta) = \frac{1}{\pi} \left[\frac{\sqrt{b^2 - (\eta - e)^2}}{y - \eta} - \sin^{-1} \frac{\eta - e}{b} + \frac{y - e}{\sqrt{b^2 - (y - e)^2}} \right.$$

$$\left. \times \ln \left| \frac{b^2 - (y - e)(\eta - e) + \sqrt{\{b^2 - (y - e)^2\}\{b^2 - (\eta - e)^2\}}}{b(y - \eta)} \right| \right]$$

$$- \frac{1}{\pi} \left[-\frac{\sqrt{b^2 - (\eta - e)^2}}{y + \eta} - \sin^{-1} \frac{\eta - e}{b} + \frac{y + e}{\sqrt{(y + e)^2 - b^2}} \sin^{-1} \frac{b^2 + (y + e)(\eta - e)}{b(y + \eta)} \right]$$

$$+ \frac{6y}{\pi} \left[-\frac{\sqrt{b^2 - (\eta - e)^2}}{(y + \eta)^2} \left\{ 1 - \frac{(y + e)(y + \eta)}{(y + e)^2 - b^2} \right\} + \frac{b^2}{\{(y + e)^2 - b^2\}^{\frac{3}{2}}} \times \sin^{-1} \frac{b^2 + (y + e)(\eta - e)}{b(y + \eta)} \right]$$

$$- \frac{2y^2}{\pi} \left[\frac{\sqrt{b^2 - (\eta - e)^2}}{(y + \eta)^3} \times \left\{ -2 + \frac{(y + e)(y + \eta)}{(y + e)^2 - b^2} + \frac{\{2b^2 + (y + e)^2\}(y + \eta)^2}{\{(y + e)^2 - b^2\}^2} \right\} \right.$$

$$\left. + \frac{3b^2(y + e)}{\{(y + e)^2 - b^2\}^{\frac{5}{2}}} \sin^{-1} \frac{b^2 + (y + e)(\eta - e)}{b(y + \eta)} \right]$$

APPENDIX 3: INFLUENCE COEFFICIENTS FOR ELLIPSE

The influence coefficients can be calculated from the stress fields for a point force X or Y acting at (ξ,η) (Appendix 1). Since the relations $d\eta = b \cos \varphi \, d\varphi$ and $-d\xi = a \sin \varphi \, d\varphi$ prevail along the ellipse, the coefficients can be expressed as[1] :

$$\sigma_{xM}^{XN} = \int_N \sigma_x^X \, (\xi,\eta,x,y)\big|_{X=1} \, b \cos \varphi \, d\varphi$$

$$\sigma_{yM}^{XN} = \int_N \sigma_y^X \, (\xi,\eta,x,y)\big|_{X=1} \, b \cos \varphi \, d\varphi$$

$$\tau_{xyM}^{XN} = \int_N \tau_{xy}^X \, (\xi,\eta,x,y)\big|_{X=1} \, b \cos \varphi \, d\varphi$$

and

$$\sigma_{xM}^{YN} = \int_N \sigma_x^Y \, (\xi,\eta,x,y)\big|_{Y=1} \, a \sin \varphi \, d\varphi$$

$$\sigma_{yM}^{YN} = \int_N \sigma_y^Y \, (\xi,\eta,x,y)\big|_{Y=1} \, a \sin \varphi \, d\varphi$$

$$\tau_{xyM}^{YN} = \int_N \tau_{xy}^Y \, (\xi,\eta,x,y)\big|_{Y=1} \, a \sin \varphi \, d\varphi$$

where $\int_N$ stands for integration of the N-th interval and σ_x^X, σ_x^Y, σ_y^X, σ_y^Y, τ_{xy}^X, τ_{xy}^Y are given in Appendix 1.

APPENDIX 4: INTEGRALS OVER SINGULARITIES FOR ELLIPSE

The integrals over the singularities for the ellipse can be approximated by the following simple analytic expressions[6] :

$$\Delta\sigma_{xM}^{XM} = \epsilon \frac{k}{4\pi (k^2 + w^2)^3} [6w^6 + (3 - 2k^2) w^4 - 6k^2w^2 - k^4]$$

$$\Delta\sigma_{yM}^{XM} = \epsilon \frac{k}{4\pi (k^2 + w^2)^3} [- 2w^6 - (1 - 6k^2) w^4 + 6k^2w^2 - k^4]$$

$$\Delta\tau_{xyM}^{XM} = \epsilon \frac{k^2}{4\pi (k^2 + w^2)^3} [- 9w^5 - (6 + 2k^2) w^3 + k^2 (2 - k^2) w]$$

$$\Delta\sigma_{xM}^{YM} = \epsilon \frac{k}{4\pi (k^2 + w^2)^3} [- w^6 + 6k^2w^4 + k^2 (6 - k^2) w^2 - 2k^4]$$

$$\Delta\sigma_{yM}^{YM} = \epsilon \frac{k}{4\pi (k^2 + w^2)^3} [- w^6 - 6k^2w^4 + k^2 (2 - k^2) w^2 + 6k^4]$$

$$\Delta\tau_{xyM}^{YM} = - \epsilon \frac{1}{4\pi (k^2 + w^2)^3} [(1 - 2k^2) w^5 + 2k^2 (1 + 3k^2) w^3 + 9k^4w]$$

where $k = b/a$

$w = \tan \varphi_0$ (φ_0 = elliptic parameter value of mid-point of M-th interval)

Note that there is a sign change from the original (Reference 6) in the expression for $\Delta\sigma_{yM}^{YM}$.

APPENDIX 5: STRESSES CLOSE TO ELLIPSE

The stresses at a point infinitesimally close to the ellipse subjected to a body force may be calculated in the following manner as given by Nisitani[4] in somewhat less detail.

Consider an elliptic arc (Fig. A1) of length 2ϵ on the x' axis. When a body force having densities $\rho_{y'}$, $\rho_{x'}$ acts on the arc, the stresses at a point $(0,b)$ (b small) due to $\rho_{x'} dx'$ and $\rho_{y'} dx'$ are obtained by differentiating the equations of the stress field in an infinite plate (Appendix 1).

$$d\sigma_{x'} = \frac{x'(3x'^2 + b^2)}{4\pi(b^2 + x'^2)^2}\rho_{x'} dx' + \frac{b(b^2 - x'^2)}{4\pi(b^2 + x'^2)}\rho_{y'} dx'$$

$$d\sigma_{y'} = -\frac{x'(x'^2 - b^2)}{4\pi(b^2 + x'^2)^2}\rho_{x'} dx' - \frac{b(3b^2 + x'^2)}{4\pi(b^2 + x'^2)^2}\rho_{y'} dx'$$

$$d\tau_{x'y'} = -\frac{b(3x'^2 + b^2)}{(b^2 + x'^2)^2}\rho_{x'} dx' + \frac{x(3b^2 + x'^2)}{(b^2 + x'^2)^2}\rho_{y'} dx'$$

Putting $x' = b\tan\theta$; $\varphi = \tan^{-1}\dfrac{\epsilon}{b}$; $dx' = b\sec^2\theta\, d\theta$ and integrating:

$$\sigma_{x'} = \frac{1}{4\pi}\int_{-\varphi}^{\varphi}\left[\sin\theta\cos\theta\left(\frac{3\sin^2\theta}{\cos^2\theta} + 1\right)\rho_{x'} + (\cos^2\theta - \sin^2\theta)\rho_{y'}\, d\theta\right]$$

$$\sigma_{y'} = \frac{1}{4\pi}\int_{-\varphi}^{\varphi}\left[-\sin\theta\cos\theta(\tan^2\theta - 1)\rho_{x'} - (3\cos^2\theta + \sin^2\theta)\rho_{y'}\right]d\theta$$

$$\tau_{x'y'} = \frac{1}{4\pi}\int_{-\varphi}^{\varphi}\left[-(3\sin^2\theta + \cos^2\theta)\rho_{x'} + \sin\theta\cos\theta(3 + \tan^2\theta)\rho_{y'}\right]d\theta$$

As b tends to zero, θ tends to $\pi/2$ and the stresses become:

$$\sigma_{x'} = 0 ; \quad \sigma_{y'} = -\frac{1}{2}\rho_{y'} ; \quad \tau_{x'y'} = -\frac{1}{2}\rho_{x'} \tag{A1}$$

Note the difference in sign of $\tau_{x'y'}$ compared with that in Reference 4.

Resolving the force densities along x and y axes as in Figure A2 gives

$$\rho_{x'} = -\rho_y \sin\theta\cos\theta + \rho_x \cos\theta\sin\theta$$

$$= \frac{1}{2}(\rho_x - \rho_y)\sin 2\theta \qquad\qquad\qquad (A2)$$

$$\rho_{y'} = \rho_y \sin^2\theta + \rho_x \cos^2\theta$$

Resolving the stresses along the x' and y' axes as in Figure A3 gives

$$\Delta\sigma_x = \sigma_{x'}\sin^2\theta + \sigma_{y'}\cos^2\theta + 2\tau_{x'y'}\sin\theta\cos\theta$$

$$\Delta\sigma_y = \sigma_{x'}\cos^2\theta + \sigma_{y'}\sin^2\theta - 2\tau_{x'y'}\sin\theta\cos\theta$$

$$\Delta\tau_{xy} = -\sigma_{x'}\cos\theta\sin\theta + \sigma_{y'}\cos\theta\sin\theta - \tau_{x'y'}(\cos^2\theta - \sin^2\theta)$$

Substituting Equations (A1) and (A2) into the above gives

$$\Delta\sigma_x = -\frac{1}{2}\cos^2\theta\,(\rho_x\cos^2\theta + \rho_y\sin^2\theta) - \frac{\sin\theta\cos\theta}{2}(\rho_x - \rho_y)\sin 2\theta$$

$$= -\frac{1}{2}\rho_x\cos^2\theta\,(1 + \sin^2\theta) + \frac{1}{2}\rho_y\,(\cos^2\theta\sin^2\theta)$$

$$= -\frac{\rho_x}{16}(5 + 4\cos 2\theta - \cos 4\theta) + \frac{\rho_y}{16}(1 - \cos 4\theta)$$

$$\Delta\sigma_y = -\frac{1}{2}\sin^2\theta\,(\rho_x\cos^2\theta + \rho_y\sin^2\theta) + \frac{\sin\theta\cos\theta}{2}(\rho_x - \rho_y)\sin 2\theta$$

$$= \frac{1}{2}\rho_x\,(\cos^2\theta\sin^2\theta) - \frac{1}{2}\rho_y\,(\sin^2\theta)(1 + \cos^2\theta)$$

$$= \frac{\rho_x}{16}(1 - \cos 4\theta) - \frac{\rho_y}{16}(5 - 4\cos 2\theta - \cos 4\theta)$$

$$\Delta\tau_{xy} = -\frac{\cos\theta\,\sin\theta}{2}\,(\rho_x\cos^2\theta + \rho_y\sin^2\theta) + \frac{(\cos^2\theta - \sin^2\theta)}{4}\,(\rho_x - \rho_y)\sin 2\theta$$

$$= -\frac{1}{2}\,\rho_x\,(\sin^3\theta\,\cos\theta) - \frac{1}{2}\,\rho_y\,(\cos^3\theta\,\sin\theta)$$

$$= -\frac{\rho_x}{16}\,(2\sin 2\theta - \sin 4\theta) - \frac{\rho_y}{16}\,(2\sin 2\theta + \sin 4\theta)$$
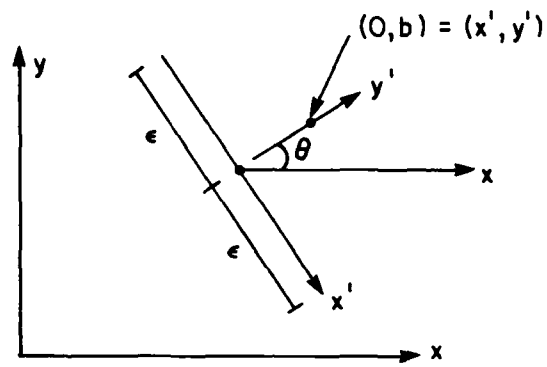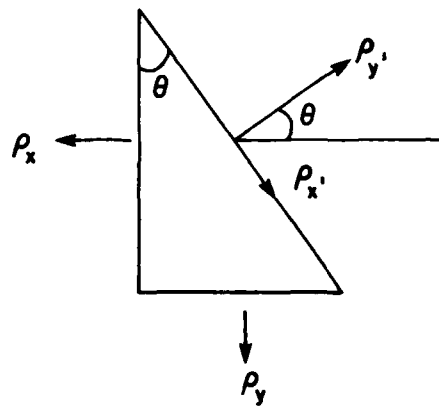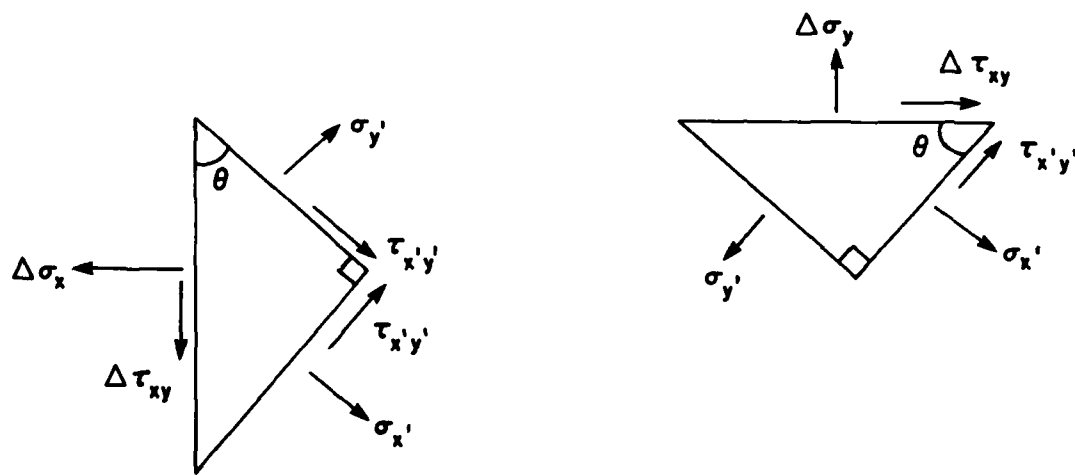
FIG. A1

FIG. A2

FIG. A3

APPENDIX 6: ADDITIONAL INFLUENCE COEFFICIENTS FOR
COMBINED CRACK AND ELLIPSE

The stresses, $\sigma_{xMe}^{\gamma N}$, $\sigma_{yMe}^{\gamma N}$ and $\tau_{xyMe}^{\gamma N}$, on the M-th interval of an ellipse due to a pair of point forces on the N-th interval of a crack are given as[7] :

$$\sigma_{xMe}^{\gamma N} = \int_N \left. \frac{\partial \sigma_x^X}{\partial \xi} \right|_{\xi=0} \sqrt{c^2 - (\eta - e)^2} \; d\eta$$

$$\sigma_{yMe}^{\gamma N} = \int_N \left. \frac{\partial \sigma_y^X}{\partial \xi} \right|_{\xi=0} \sqrt{c^2 - (\eta - e)^2} \; d\eta$$

$$\tau_{xyMe}^{\gamma N} = \int_N \left. \frac{\partial \tau_{xy}^X}{\partial \xi} \right|_{\xi=0} \sqrt{c^2 - (\eta - e)^2} \; d\eta$$

where

$$\left. \frac{\partial \sigma_x^X}{\partial \xi} \right|_{\xi=0} = \frac{1}{4\pi y^2 (A^2 + m^2)^3} [-3A^4 + 6A^2m^2 + m^4] + \frac{1}{4\pi y^2 (A^2 + n^2)^4}$$

$$\times [-5A^6 + (13n^2 + 12n - 12) A^4 + n^2 (17n^2 - 72n + 72) A^2 - n^4 (n^2 - 12n + 12)]$$

$$\left. \frac{\partial \sigma_y^X}{\partial \xi} \right|_{\xi=0} = \frac{1}{4\pi y^2 (A^2 + m^2)^3} [A^4 - 6A^2m^2 + m^4] + \frac{1}{4\pi y^2 (A^2 + n^2)^4}$$

$$\times [-A^6 + (5n^2 - 36n + 12) A^4 + n^2 (5n^2 + 56n - 72) A^2 - n^4 (n^2 + 4n - 12)]$$

$$\left. \frac{\partial \tau_{xy}^X}{\partial \xi} \right|_{\xi=0} = \frac{Am}{2\pi y^2 (A^2 + m^2)^3} [-3A^2 + m^2] + \frac{1}{4\pi y^2 (A^2 + n^2)^4}$$

$$\times [2 (3n + 2) A^5 + 4n (n^2 - 14n + 12) A^3 - 2n^3 (n^2 - 18n + 24) A]$$

and
$$A = -\frac{x}{y}, \quad m = \frac{\eta - y}{y}, \quad n = \frac{\eta + y}{y}$$

Note the change of sign in $\dfrac{\partial \tau_{xy}^X}{\partial \xi}$ as compared to the equation given in Reference 7.

The stresses, σ_{xMc}^{XN} and σ_{xMc}^{YN} on the M-th crack interval due to point forces on the N-th elliptic interval are

$$\sigma_{xMc}^{XN} = \sigma_{xMe}^{XN}\bigg|_{x=0} \; ; \quad \sigma_{xMc}^{YN} = \sigma_{xMe}^{YN}\bigg|_{x=0}$$

(see Appendix 3).

REPORT DOCUMENTATION PAGE / PAGE DE DOCUMENTATION DE RAPPORT

REPORT/RAPPORT	REPORT/RAPPORT
NAE-AN-17	NRC No. 22831
1a	1b

REPORT SECURITY CLASSIFICATION CLASSIFICATION DE SÉCURITÉ DE RAPPORT	DISTRIBUTION (LIMITATIONS)
Unclassified	Unlimited
2	3

TITLE/SUBTITLE/TITRE/SOUS-TITRE
Implementation of Nisitani's Body Force Method for the Solution of Notch Problems

4

AUTHOR(S)/AUTEUR(S)

W.E. Fraga, R.L. Hewitt

5

SERIES/SÉRIE

Aeronautical Note

6

CORPORATE AUTHOR/PERFORMING AGENCY/AUTEUR D'ENTREPRISE/AGENCE D'EXÉCUTION
National Research Council Canada
National Aeronautical Establishment   Structures and Materials Laboratory

7

SPONSORING AGENCY/AGENCE DE SUBVENTION

8

DATE	FILE/DOSSIER	LAB. ORDER COMMANDE DU LAB.	PAGES	FIGS/DIAGRAMMES
83-11			53	18
9	10	11	12a	12b

NOTES

13

DESCRIPTORS (KEY WORDS)/MOTS-CLÉS
1. Boundary integral method
2. Stress intensity factors
3. Stress concentration

14

SUMMARY/SOMMAIRE

An outline of Nisitani's body force method is presented and details of the numerical implementation provided. Full details are provided for the solution of several problems including single cracks or single elliptical notches in semi-infinite plates as well as the problem of an embedded crack near a semi-elliptical notch in a semi-infinite plate.

15

END

FILMED

3-84

DTIC